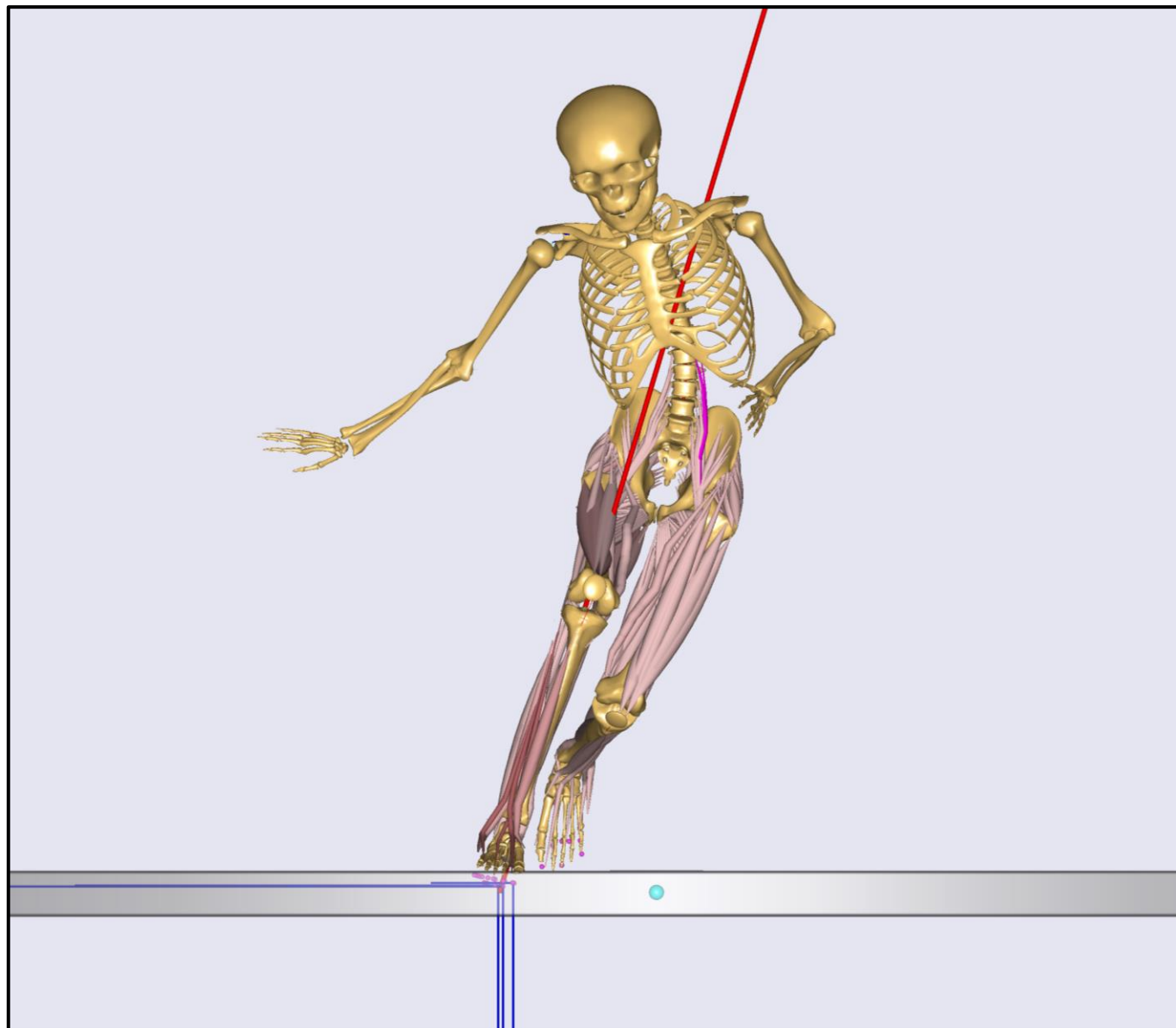# Prediction of ground reaction forces and moments during sports-related movements

Sebastian Laigaard Skals

Master's Thesis submitted 2nd June 2015

Master of Sports Technology
Department of Health Science and Technology
Aalborg University

Supervisors

Michael Skipper Andersen

Miguel Nobre Castro

AALBORG UNIVERSITY

Prediction of ground reaction forces and moments during sports-related movements

Sebastian Laigaard Skals

Department of Health Science and Technology, Aalborg University, Aalborg, Denmark

Abstract

Inverse dynamic analysis (IDA) on musculoskeletal models has become a commonly used method to study human movement. However, when solving the inverse dynamics problem, inaccuracies in experimental input data and a mismatch between model and subject leads to dynamic inconsistency. By predicting the ground reaction forces and moments (GRF&Ms), this inconsistency can be reduced and force plate measurements become unnecessary. In this study, a method for predicting the GRF&Ms was adopted and validated for an array of sports-related movements. The method uses a scaled musculoskeletal model and the equations of motion alone to predict GRF&Ms from full-body motion, and entails a dynamic contact model and optimization techniques to solve the indeterminacy during double support. The method was applied to ten healthy subjects performing e.g. running, a side-cut manoeuvre and vertical jump. Pearson's correlation coefficient (r) was used to compare the predicted GRF&Ms and associated joint kinetics to the corresponding variables obtained from a traditional IDA approach, where the GRF&Ms were measured using force plates. In addition, peak vertical GRFs and resultant JRFs were computed and statistically compared. The main findings were that the method provided estimates comparable to the traditional IDA approach for vertical GRFs (r ranging from 0.96 to 0.99, median 0.99), joint flexion moments (r ranging from 0.79 to 0.98, median 0.93) and resultant JRFs (r ranging from 0.78 to 0.99, median 0.97), across all movements. Although discrepancies were identified for some variables and the majority of the peak forces were significantly different, the former were mainly contributed to noise while the differences in peak forces could potentially be overcome by adjusting parameters in the contact model. Considering these results, this method could be used instead of force plate data, hereby facilitating IDA in sports science research and providing valuable opportunities for complete IDA using motion analysis systems that does not commonly incorporate force plate data, such as marker-less motion capture.

Keywords: *Ground reaction forces and moments, musculoskeletal model, inverse dynamics, sports-related movements, validation*

1. Introduction

Musculoskeletal modelling is an important tool towards understanding the internal mechanisms of the body during various movements and loading conditions, which are otherwise impractical or impossible to measure. To this day, it remains very challenging to measure muscle, ligament and joint forces in vivo and the associated procedures are invasive. Therefore, the use of simulation models to estimate these variables has become widespread and contribute important information to a variety of scientific fields, such as clinical gait analysis (Zajac et al., 2003; Vaughan et al., 1999), ergonomics (Rasmussen et al., 2003a, 2003b), orthopaedics (Mellon et al., 2013, 2015; Weber et al., 2014) and sports biomechanics (Payton and Bartlett, 2008).

There exist a number of different analytical approaches within the area of musculoskeletal modelling. Firstly, *Forward Dynamics-based tracking methods* use computed muscle control, which is held up against measured kinematics to determine the muscle actions that produce a given motion (Thelen and Anderson, 2006). Secondly, *EMG-driven forward dynamics* estimates the contribution of individual muscles during motion using a combination of kinematic and electromyographic data (Barret et al., 2007). Thirdly, *Dynamic Optimization* involves defining the goal of the motor task and applying an optimization approach to compute the motor patterns and kinematics (Anderson and Pandy, 2001). Finally, *Inverse Dynamics* approaches the problem from the opposite end and determines the muscle and joint forces from kinematic and/or external force data (Erdemir et al., 2007; Damsgaard et al., 2006). More specifically, measurements of body motion and external forces are input to the equations of motion and the joint reaction and muscle forces can be computed in a process known as muscle recruitment (Damsgaard et al., 2006; Rasmussen et al., 2001).

Typically, marker-based motion analysis and force plate measurements are used to determine body segment kinematics (i.e., positions, velocities and accelerations) (Andersen et al., 2009; Cappozzo et al., 2005) and ground reaction forces and moments (GRF&Ms) (Nigg, 2006), respectively, while the body segment parameters (i.e., segment mass, centre-of-mass and moment-of-inertia) are determined through cadaver-based studies (Carbone et al., 2015; Horsman et al., 2007; Clauser et al., 1969) and model scaling techniques (Lund et al., 2015; Andersen et al., 2010). However, it is well-known that the results of inverse dynamic analysis (IDA) are sensitive to inaccuracies in these input data (Pámies-Vila et al., 2012; Riemer et al., 2008). Inaccuracies can stem from multiple sources, such as estimating joint (Schwartz et al., 2005) and body segment parameters (Rao et al., 2006; Pearsall and Costigan, 1999), marker sliding relative to the underlying bone due to soft tissue artefacts (Leardini et al., 2005; Stagni et al., 2005), marker misplacement (Della Croce et al., 2005), camera-system (Chiari et al., 2005) and force plate calibration (Collins et al.,

2009), determining centre-of-pressure (Middleton et al., 1999) and variability in force plate data (Psycharakis and Miller, 2006). In addition, there exists a fundamental mismatch between the measurements obtained from the real biosystem and the mathematical model used for analysis (Hatze, 2002). When analysing full-body models, the system becomes over-determinate as the GRF&Ms are input to the equations of motion (Cahouët et al., 2002; Hatze, 2002; Kuo, 1998). In some cases, it can be justifiable to solve the overdeterminacy by simply discarding acceleration measurements for one or more segments in the model. When this is not possible, however, the dynamic inconsistency arising from system overdeterminacy and experimental input inaccuracies can be solved by introducing residual forces and moments in the model to obtain dynamic equilibrium (Fluit et al., 2014a; Cahouët et al., 2002; Kuo, 1998).

In order to improve dynamic consistency, these residual forces and moments have been used to reduce error effects from the input data through various optimization methods (Riemer and Hsiao-Wecksler, 2008; Delp et al., 2007; Cahouët et al., 2002; Kuo, 1998; Vaughan et al., 1982). Alternatively, dynamic consistency can be improved by deriving the GRF&Ms from the model kinematics and segment dynamical properties only, which is commonly known as the top-down approach (Riemer and Hsiao-Wecksler, 2008; Cahouët et al., 2002). The application of the top-down approach has traditionally been limited by the fact that the inverse dynamics problem becomes indeterminate during double contact phases, where the system forms a closed kinetic chain (Fluit et al., 2014a; Audu et al., 2007). In recent years, however, several studies have provided solutions to this issue (Fluit et al., 2014a; Choi et al., 2013; Eel Oh et al., 2013; Robert et al., 2013; Ren et al., 2008; Audu et al., 2007; Audu et al., 2003). Most recently, Fluit et al. (2014a) demonstrated a universal method for predicting GRF&Ms using kinematic data and a scaled musculoskeletal model only. The indeterminacy issue during double contact was solved by employing a dynamic contact model and optimization techniques. Specifically, the researchers introduced five artificial muscle-like actuators at 12 contact points under each foot in the model and computed the GRF&Ms as part of the muscle recruitment algorithm. The method was validated against measured data for an array of activities of daily living, such as gait, deep squatting and stair ascent, and reasonably good results were obtained for all analysed activities.

Besides improving dynamic consistency, predicting rather than measuring GRF&Ms obviates the need for force plate measurements, which has some additional advantages. 1) The measurement errors associated with force plates can be eliminated. 2) Force plate targeting can be avoided; an issue that may affect the resulting segment angles and GRF&Ms (Challis, 2001). 3) It facilitates IDA of movements that are continuous and occupy a large space (Choi et al., 2013). 4) GRF&Ms can be obtained in outdoor environments without having to instrument force plates. Currently, motion analysis systems exist that are

able to operate in outdoor environments, but force plates are difficult and expensive to install in multi-settings (Choi et al., 2013) and are sensitive to temperature and humidity variations (Psycharakis and Miller, 2006). For sports science research, 3 and 4 are particularly advantageous. Ensuring force plate impact during motions that are highly dynamic and require large amounts of space can be difficult, which is the case for many movements associated with sports. This can potentially restrict natural execution of the motion or even require force plate targeting to ensure impact, which could compromise the quality of the measurements. In addition, many sports-related movements can only be analysed in their entirety by performing measurements outdoors, which is currently infeasible using force plates. However, none of the existing methods for predicting GRF&Ms have been validated for sports-related movements.

Therefore, the goal of this study was to evaluate the accuracy of the method proposed by Fluit et al. (2014a) to predict GRF&Ms during sports-related movements. This was accomplished by performing IDA on a variety of movements, such as running, vertical jump and a side-cut manoeuvre. For validation, the predicted GRF&Ms and associated joint kinetics were compared with the corresponding values from the model, in which GRF&Ms were obtained using force plates. If comparable accuracy between these two methods can be established, it would provide new and valuable opportunities for IDA in sports science research.

2. Materials and methods

2.1 Experimental procedures

Ten healthy subjects (8 males and 2 females, age: 25.70 ± 1.49 years, height: 180.80 ± 7.39 cm, weight: 76.88 ± 10.37 kg) volunteered to participate in the study and provided written informed consent. The study was conducted at the Department of Health Science and Technology, Aalborg University, Aalborg, Denmark.

During measurements, male subjects exclusively wore tight fitting underwear or running tights, while female subjects also wore a sports-brassiere. In addition, all subjects wore a pair of running shoes in their preferred size, specifically the *Brooks Ravenna 2* (Brooks Sports Inc., Seattle, WA, US). This decision was made in order to minimize discomfort and, hereby, facilitate a more natural execution of the movements. Initially, a 5 min warm-up at 160 W was completed on a cycle ergometer before multiple practice trials were performed. The practice trials served two overall purposes and were preceded by a thorough instruction. First, some of the included movements were considered technically challenging and required multiple repetitions to ensure consistent technique throughout the duration of the experiment.

4

Furthermore, it was desired to obtain some degree of technical consistency between subjects to reduce variability in the resulting measurements. Second, the starting position for each movement was established through trial-and-error until the subjects were able to consistently impact the force plates. When it was assessed that the subjects were consistently able to perform the movements with adequate technique and impact the force plates accurately, their starting position was marked and they were given a brief pause before markers were taped to their skin.

The following movements were included in the study: 1) Running at a comfortable pace, 2) backwards running, 3) a side-cut manoeuvre, 4) vertical jump, and 5) accelerating from a standing position (ASP), imitating the initiation of running. These movements were chosen, as they represent some of the most common movements associated with sports and can be performed without specialised skills. In addition, the movements provided varied characteristics in the resulting GRF&Ms, considering factors such as force plate impact time, force magnitude and direction as well as providing single and double contact phases. Initially, all running trials were completed. Subjects were instructed to run at a comfortable self-selected pace and impact the force plate with their right foot, aimed towards facilitating a natural running style and a consistent pace between trials. For the side-cut manoeuvre, subjects were instructed to perform a slowly paced run-up, impact the centre of the force plate with their right foot, and accelerate to their left-hand side while targeting a cone. The centre of the force plate was marked with white tape and the cone was placed 2 m from the tape mark, angled at 45 degrees from the initial running direction. Backwards running was executed at a self-selected pace and the subjects had to impact the force plate with their right foot. During practice trials, the starting position had been established where the subjects were able to impact the force plate accurately and consistently. As a result, the subjects only had to focus on executing the movement with consistent technique, while keeping their focus straight ahead, i.e., away from the running direction, during measurements. Vertical jump was performed as a counter-movement jump, initiated with the subjects standing with each foot on separate force plates. They were asked to keep their hands fixated on the hips, focus straight ahead for the entirety of the movement cycle and refrain from excessive hip flexion. While complying with these constraints, they were asked to push-off with their legs at maximal capacity and attempt to achieve their maximal jump height. Finally, ASP was initiated with the subjects' feet separated in the sagittal plane and placed on separate force plates, while their arms were positioned inversely to their feet, closely resembling a natural initiation of running. From this position, they were asked to accelerate to their comfortable running pace. Five trials were completed for all movements, each consisting of one full movement cycle. Videos showing the executions of each movement are provided as supplementary material (Sup. Video 1-5).

2.2 Data collection

A total of 35 reflective markers were placed on the subjects, consisting of 29 markers placed on the skin surface and three markers placed on each running shoe, resembling the position of the first and fifth metatarsal and the top of the calcaneus bone. No markers were placed on the head. Further details regarding the marker protocol are provided as appendix. Marker trajectories were tracked using a marker-based motion capture system, consisting of eight infrared high-speed cameras (Oqus 300 series), sampling at 250 Hz, combined with Qualisys Track Manager v. 2.9 (Qualisys, Gothenburg, Sweden). GRF&Ms were obtained at 2000 Hz using two force plates (width/length = 464/508 mm) (Advanced Mechanical Technology, Inc., Watertown, MA, US), which were embedded in the laboratory floor.

2.3 Data processing

3-D marker trajectories and force plate data were low-pass filtered using second order, zero-phase Butterworth filters with a cut-off frequency of 15 and 10 Hz, respectively. For all movements, three of the five successful trials were included for further analysis, yielding a total of 150 trials used to validate the predicted GRF&Ms and the associated joint kinetics. Trials were excluded due to occasional marker occlusion or inadequate impact of the force plates, i.e., the whole foot was not in complete contact or the impact occurred too close to the edges of the force plate surface.

2.4 Prediction of GRF&Ms

The prediction of GRF&Ms was enabled by partly adopting the method of Fluit et al. (2014a). However, some key alterations where made to the method, which are specified in the following. The GRF&Ms were predicted by creating five artificial muscle-like actuators at 18 contact points defined under each foot of the musculoskeletal model (Figure 1). In order to compensate for the sole thickness of the running shoes and the soft tissue under the heel, the contact points on the heel were offset by 35 mm and all other points offset by 25 mm from the model bone geometry. Of the five actuators, one actuator was aligned with the vertical axis of the force plates (Z-axis) and generated a normal force. The other actuators were defined in two pairs that were aligned with the medio-lateral (X-axis) and antero-posterior axis (Y-axis) of the force plates, and were able to generate positive and negative static friction forces (with a friction coefficient of 0.5).

To establish ground contact, a dynamic contact model was applied to determine the activation level of each actuator. This approach ensured that each actuator would only generate a contact force if their associated contact point, p, was sufficiently close to the floor and almost without motion. The maximal strength of each actuator was set to $F_{max} = 0.4\,BW$, the activation threshold distance from p to the
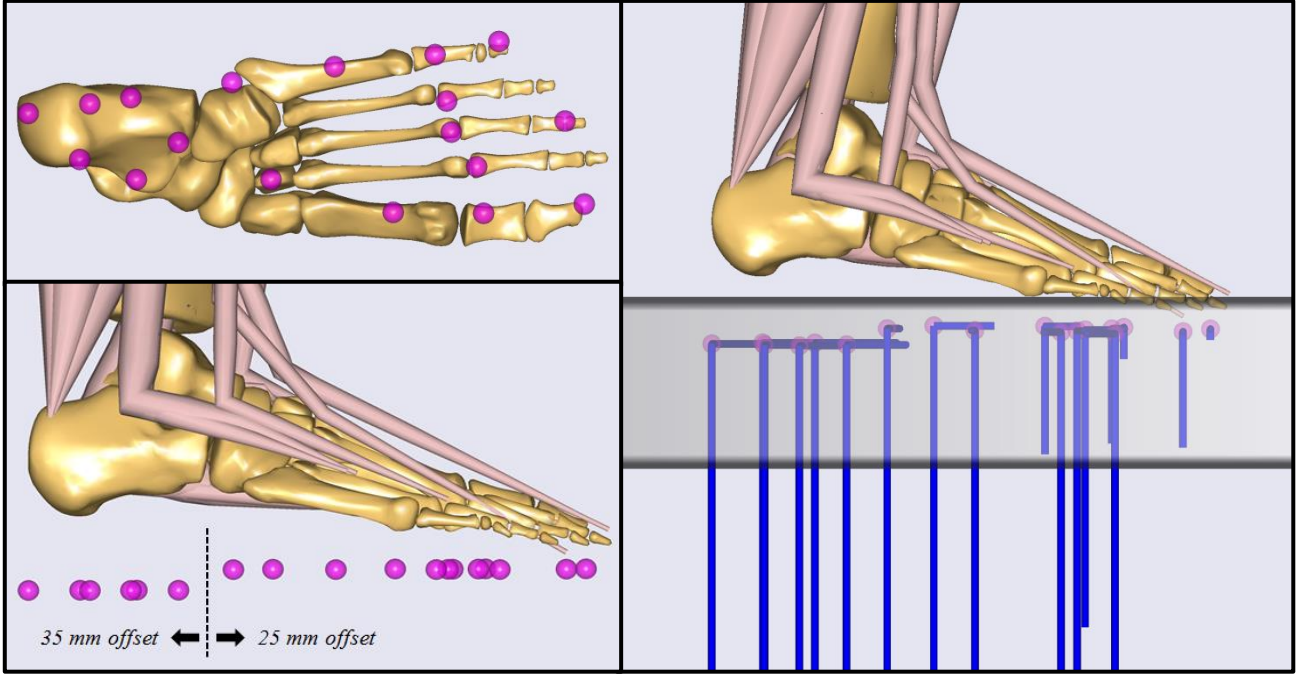
Figure 1 – Location of the contact points under the foot of the musculoskeletal model (top left), side-view of the contact points specifying the offset distances (bottom left) and the point activation after established ground contact (right).

ground plane was set to $z_{limit} = -0.01\ m$, and the activation threshold velocity of p was set to $v_{limit} = 1.3\ m/s$. In order to be activated, each contact point had to overlap with a user-defined artificial ground plane in the model environment, as illustrated in Figure 1. The specified distance, z_{limit}, represent the location of the artificial ground plane relative to the origin of the global reference frame and not the actual location of the ground. To determine the strength profile of each contact point, a nonlinear strength function was defined as

$$c_{p,i} = \begin{cases} F_{max} & if \quad z_{ratio} \le 0.8\ and\ v_{ratio} \le 0.15 \\ F_{smooth} & if \quad 0.8 \le z_{ratio} < 1\ and\ 0.15 \le v_{ratio} < 1 \\ 0 & otherwise \end{cases} \qquad (1)$$

$$where \qquad z_{ratio} = \frac{p_z}{z_{limit}}$$

$$and \qquad v_{ratio} = \frac{p_{vel}}{v_{limit}}$$

where p_z and p_{vel} defined the height and velocity of each contact point relative to the ground, respectively. Eq. (1) specifies that each actuator would assume the strength F_{max} if the associated p reached z_{limit} and v_{limit}. However, in order to prevent discontinuities in the predicted GRF&Ms due to the sudden transition of p from inactive to fully active, a smoothing function was defined as

$$F_{smooth} = F_{max}\ z_{smooth}v_{smooth} \qquad (2)$$

$$where \qquad z_{smooth} = 0.5 \left(\cos \left(\frac{z_{ratio} - 0.8}{(1 - 0.8)\pi} \right) + 1 \right)$$

$$and \qquad v_{smooth} = 0.5 \left(\cos \left(\frac{v_{ratio} - 0.15}{(1 - 0.15)\pi} \right) + 1 \right)$$

that would be assumed when p was near z_{limit} and v_{limit}, as specified in Eq. (1). Hence, the activation level of the actuators would build up gradually until the threshold values were reached. The magnitudes of the predicted GRF&Ms were determined by solving the activation level of each muscle-like actuator as part of the muscle recruitment algorithm. The solver did not distinguish between single and double contact phases, hereby providing a solution to the problem of underdeterminacy.

2.5 Musculoskeletal model

The musculoskeletal models were developed in the AnyBody Modeling System v. 6.0.4 (AMS) (AnyBody Technology A/S, Aalborg, Denmark) based on the *GaitFullBody* template from the AnyBody Managed Model Repository v. 1.6.3 (Figure 2 and 3). In the *GaitFullBody* template, the lower extremity model is based on the cadaver dataset of Horsman et al. (2007), the lumbar spine model based on the work of de Zee et al. (2007), and the shoulder and arm models based on the work of the Delft Shoulder Group (Veeger et al., 1991, 1997; Van der Helm, 1992). The model had a total of 27 degrees-of-freedom (DOF), including 2x1 DOF at the ankle joints, 2x1 DOF at the knee joints, 2x3 DOFs at the hip joints, 6 DOFs at the pelvis, 3 DOFs at the pelvis-thorax joint, 2x1 DOF at the elbow joints, and 2x3 DOFs at the glenohumeral joints. As there were no markers placed on the head, the neck joint was fixed in a neutral position.

Model scaling and kinematic analysis were performed applying the methods of Andersen et al. (2009, 2010). During the experiment, the subjects had performed multiple gait trials of which a single trial for each subject was initially used to determine segment lengths and model marker positions. These parameters were estimated by minimising the least-square difference between model and experimental markers using the method of Andersen et al. (2010), incorporating a linear-scaling law. The segment lengths and marker positions obtained from the gait trials were subsequently saved and used for the analysis of all other trials. Specifically, the optimised parameters were loaded and the least-square difference between model and experimental markers minimised over the whole trial duration to obtain the model kinematics (Andersen et al., 2009). Further details regarding the marker optimization procedure is provided as appendix.

The lower extremity model included a total of 110 constant strength muscles divided into 318 individual muscle paths, i.e., 55 muscles and 159 muscle paths for each leg, whereas ideal joint torque generators were used for the upper extremities. In addition, additional muscle-like actuators were added to
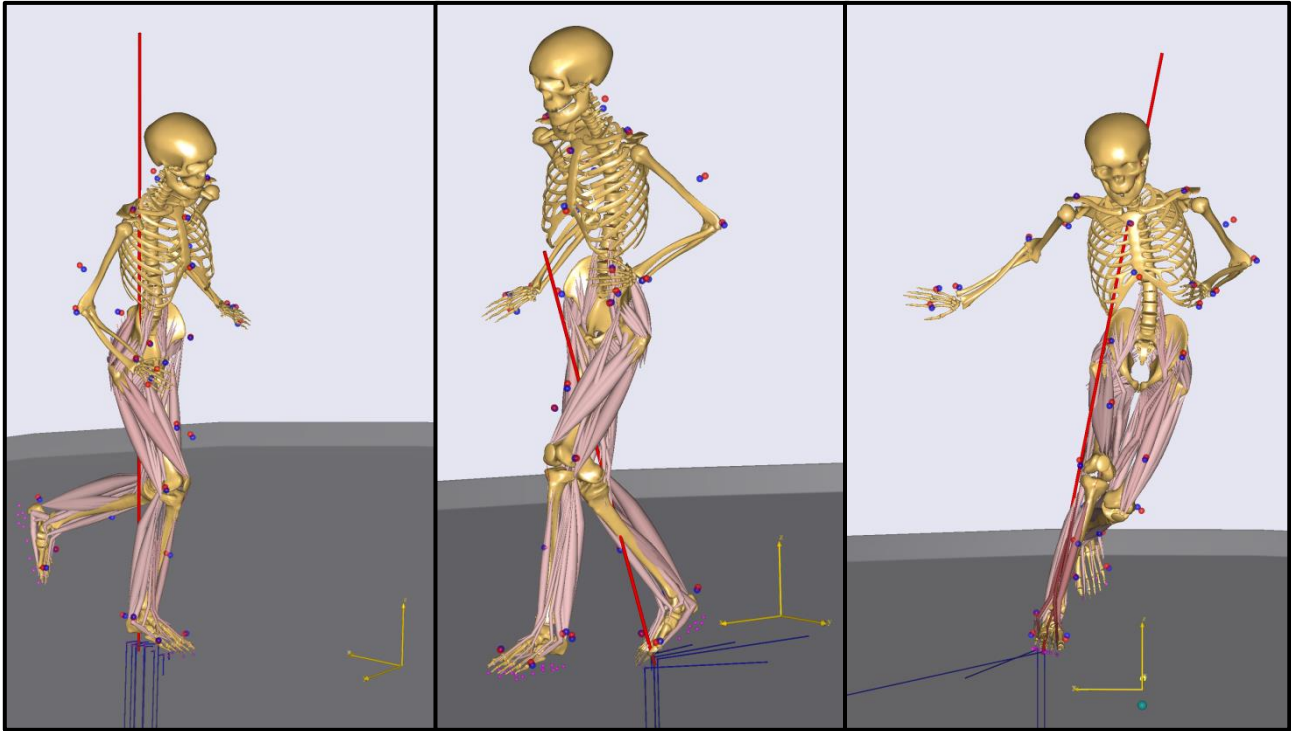
Figure 2 – Musculoskeletal models of a subject performing running (left), backwards running (centre) and a side-cut manoeuvre (right).
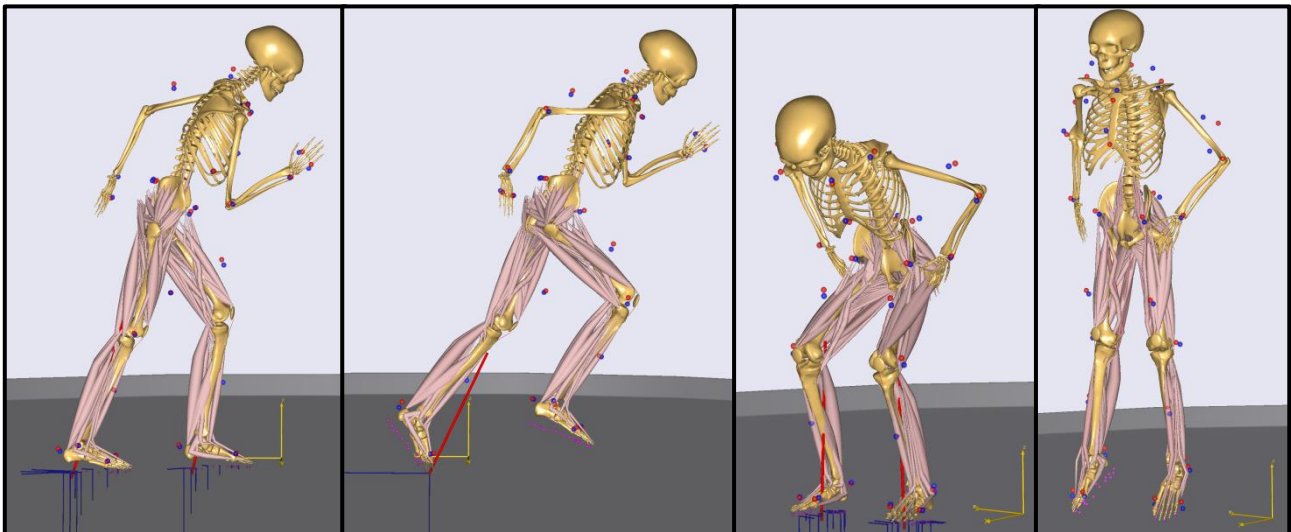

Figure 3 – From left to right: Musculoskeletal models of a subject performing ASP (initiation of the movement and near toe-off) and vertical jump (counter-movement and past toe-off).

the origin of the pelvis segment, which were able to generate residual forces and moments up to 10 N or Nm. The activation levels of these muscles were solved as part of the muscle recruitment, aimed towards minimizing their contribution. This approach was utilized in order to improve numerical stability. The muscle recruitment problem was solved by minimizing the sum of the squared muscle activities (the ratio between muscle forces and maximal isometric strengths), also known as *Quadratic muscle recruitment*, hereby, providing the muscle forces and thus the predicted GRF&Ms. The skeletal muscles and muscle-like

actuators were weighted equally during recruitment, but the strength of the actuators associated with the GRF&Ms were high compared to the skeletal muscles, whereas the strength of the residuals were relatively low.

2.6 Data analysis

For the running, backwards running and side-cut trials, data were analysed from the first foot-force plate contact instant to the last frame of contact. Vertical jump trials were analysed in the 800 ms up till toe-off, which included the complete counter-movement cycle. ASP trials were analysed in the 600 ms up till toe-off of the rear foot. The following variables were included in the analysis: Antero-posterior ground reaction force (GRF), medio-lateral GRF, vertical GRF, sagittal ground reaction moment (GRM), frontal GRM, transverse GRM, ankle flexion moment (AFM), knee flexion moment (KFM), hip flexion moment (HFM), hip abduction moment (HAM), hip external rotation moment (HERM), ankle resultant joint reaction force (JRF), knee resultant JRF and hip resultant JRF. In addition, peak resultant JRF for the ankle, knee and hip, and peak vertical GRF were computed. For the running, backwards running and side-cut trials, the selected variables were analysed for the right leg only, i.e., the stance phases of the movement cycles. For the vertical jump and ASP trials, the variables were analysed for the right and left leg separately.

In order to assess the accuracy of the predicted GRF&Ms and the associated joint kinetics, these data were compared to the corresponding variables in the model where the GRF&Ms were obtained through force plate measurements. Pearson's correlation coefficient (r) and root-mean-square deviation (RMSD) were computed to compare the selected variables. Following the procedures of Taylor (1990), the absolute values of r were categorized as weak, moderate, strong and excellent for $r \leq 0.35$, $0.35 < r \leq 0.67$, $0.67 < r \leq 0.90$, $0.90 < r$, respectively. To test the differences between the computed peak GRFs and peak resultant JRFs associated with each approach, Wilcoxon paired-sample tests were applied for which $p < 0.05$ are reported as a significant difference.

3. Results

The time-histories of the selected variables for running, backwards running and side-cut are depicted in Figures 4-7 (a), and vertical jump and ASP trials are depicted in Figures 4-7 (b). The results of the statistical analysis and the RMSD for running, backwards running, and side-cut are summarized in Tables 1-3 (a), while the results for vertical jump and ASP are summarized in Tables 1-3 (b). For the majority of the variables, comparable results were observed between datasets. Across all movements, excellent correlations were found for vertical GRF (r ranging from 0.96 to 0.99, median 0.99), and strong to excellent correlations were found for sagittal GRM (r ranging from 0.69 to 0.95, median 0.87), all joint flexion moments (r ranging from
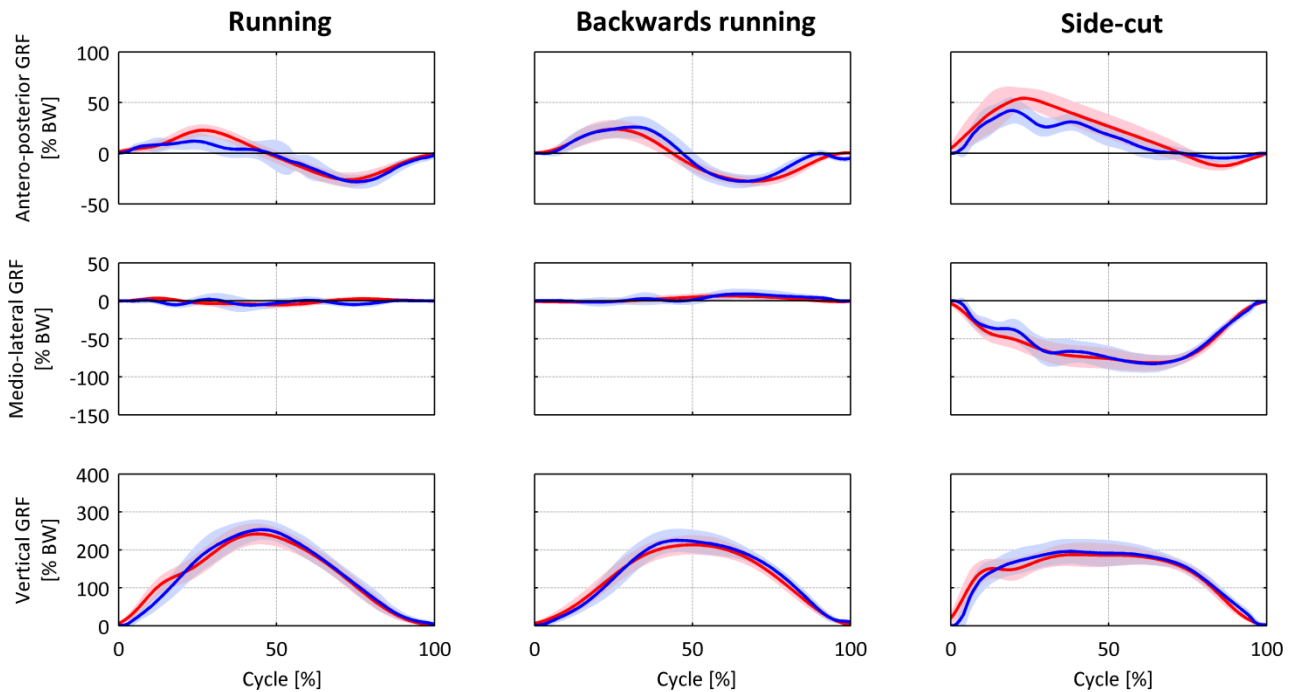
Figure 4 (a) – Results for running, backwards running and side-cut, illustrating antero-posterior GRF, medio-lateral GRF and vertical GRF. The predicted variables are illustrated in blue and the measured variables in red. The results are presented as the mean ± 1 SD (shaded area).
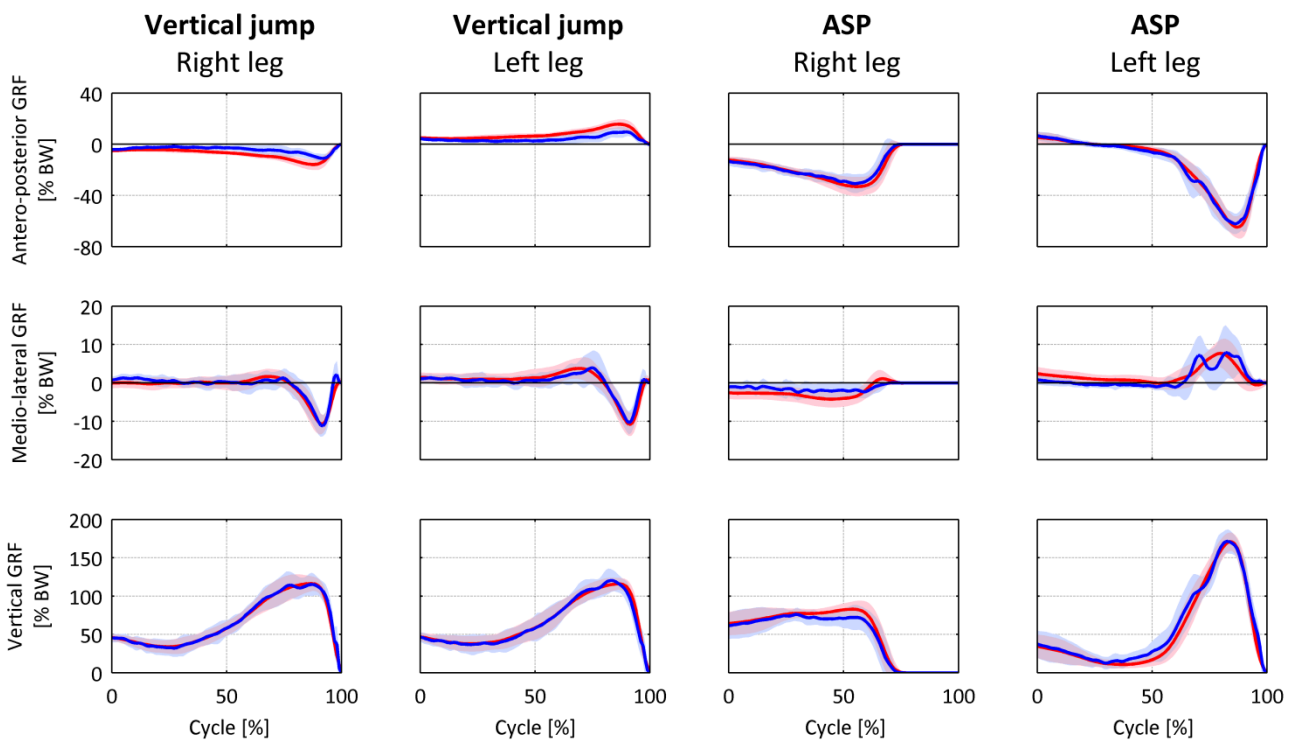

Figure 4 (b) – Results for vertical jump and accelerate from standing position (ASP), illustrating antero-posterior GRF, medio-lateral GRF and vertical GRF. The predicted variables are illustrated in blue and the measured variables in red. The results are presented as the mean ± 1 SD (shaded area).
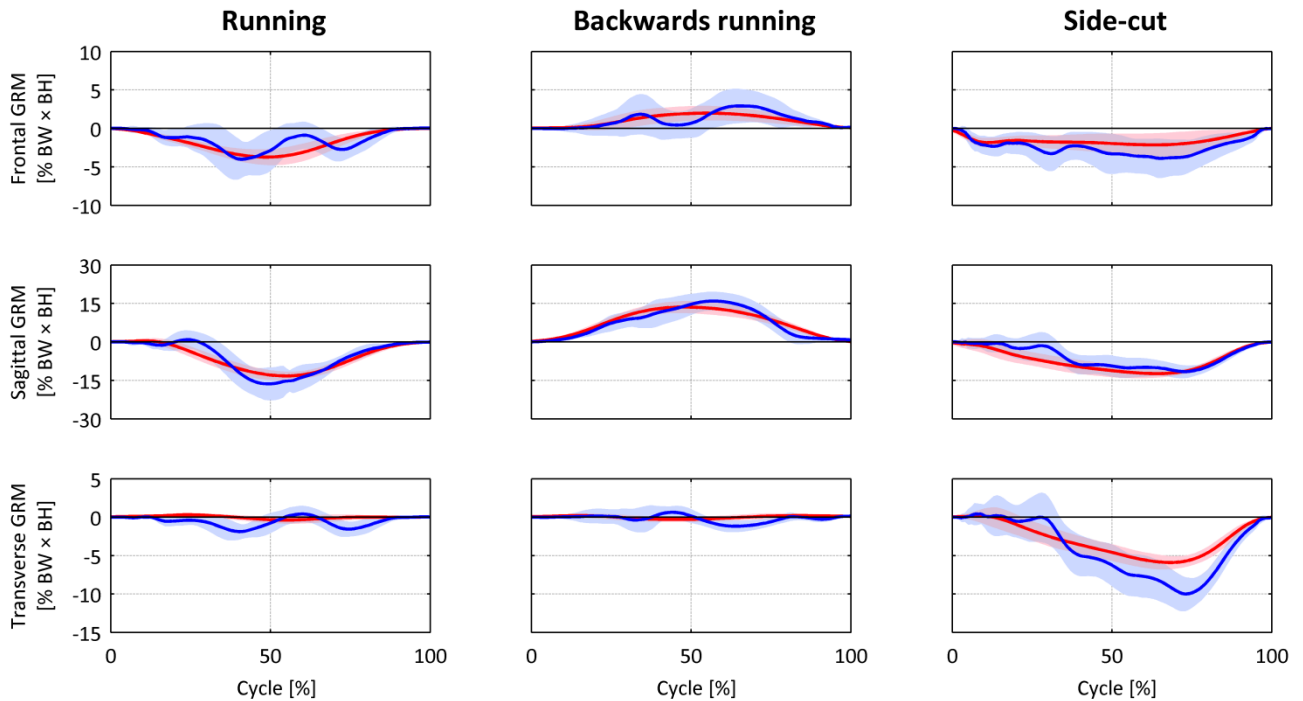
Figure 5 (a) – Results for running, backwards running and side-cut, illustrating frontal GRM, sagittal GRM and transverse GRM. The predicted variables are illustrated in blue and the measured variables in red. The results are presented as the mean ± 1 SD (shaded area).
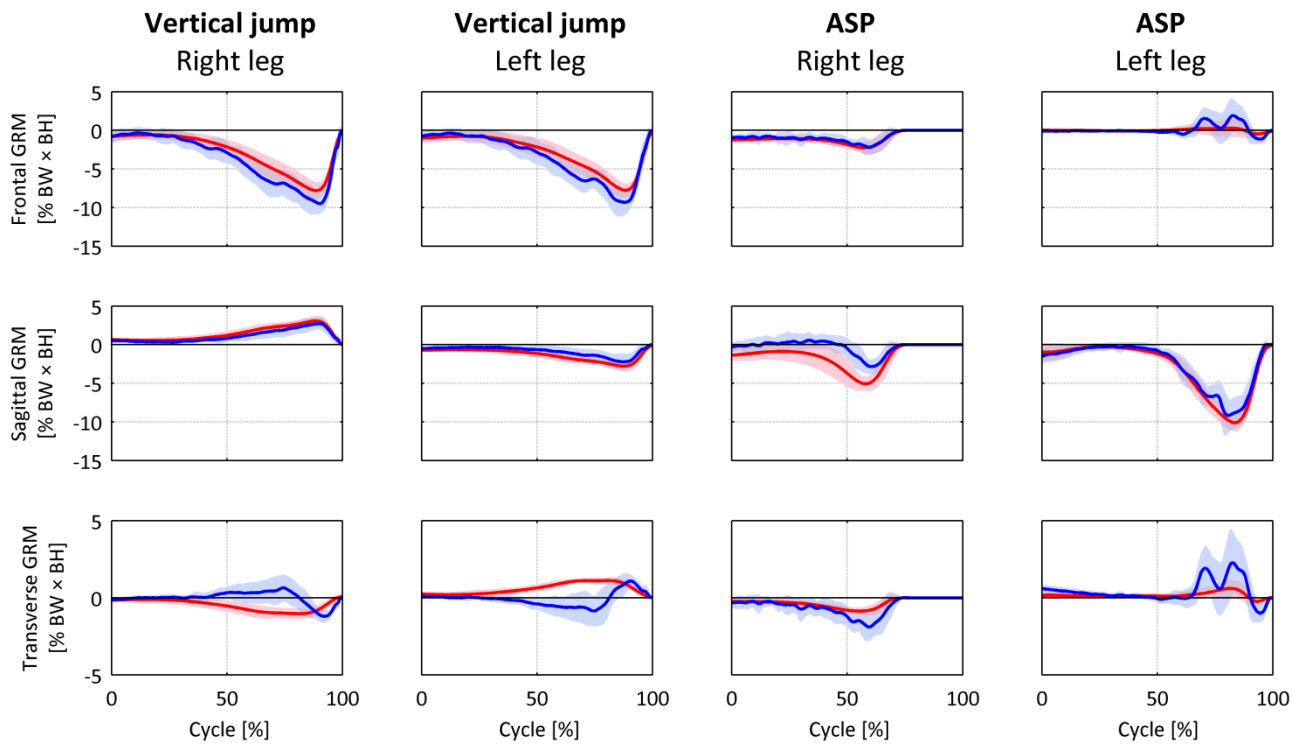

Figure 5 (b) – Results for vertical jump and accelerate from standing position (ASP), illustrating frontal GRM, sagittal GRM and transverse GRM. The predicted variables are illustrated in blue and the measured variables in red. The results are presented as the mean ± 1 SD (shaded area).
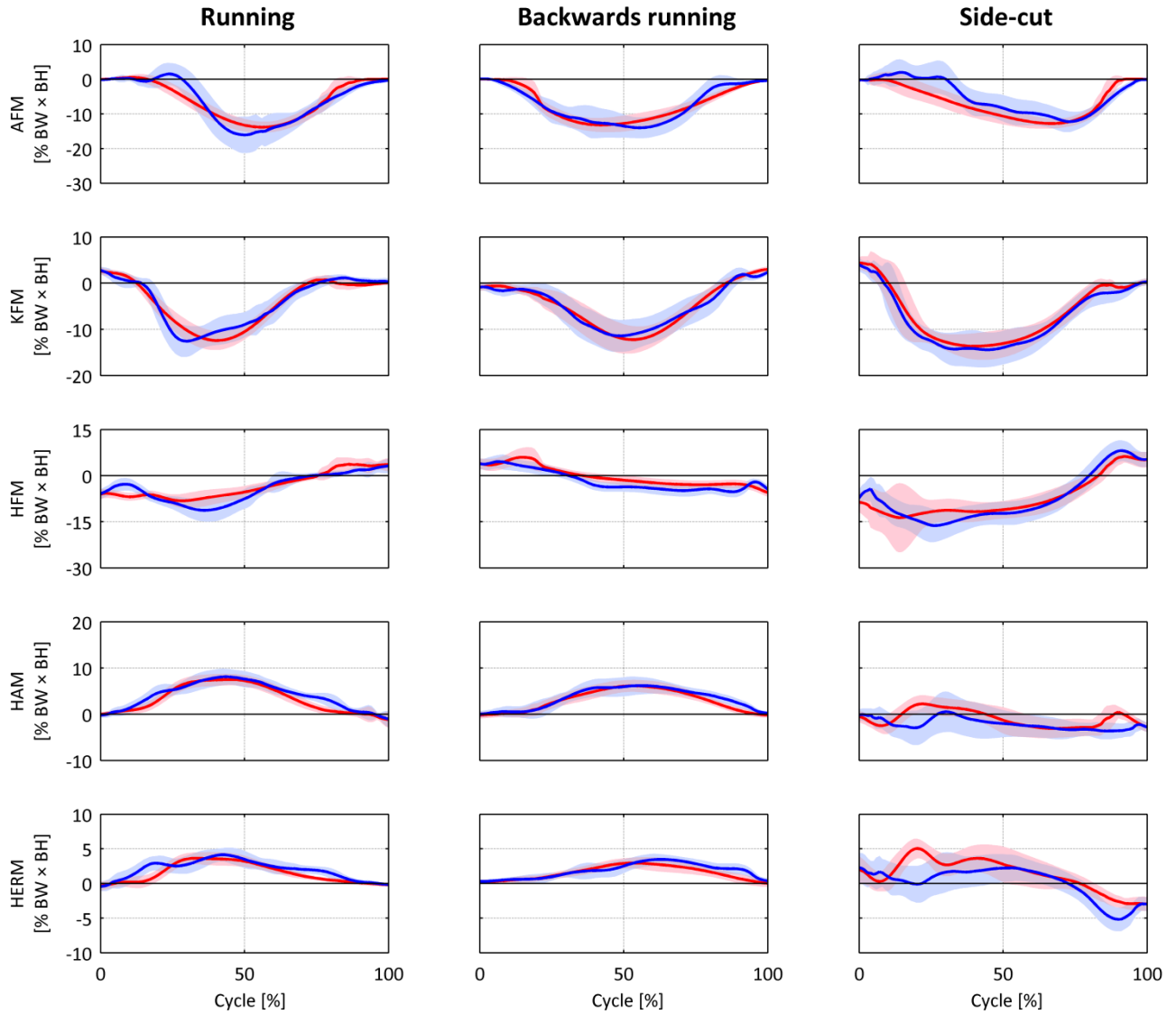
Figure 6 (a) – Results for running, backwards running and side-cut, illustrating ankle (AFM), knee (KFM) and hip flexion moment (HFM), hip abduction moment (HAM) and hip external rotation moment (HERM). The variables associated with the predicted and measured GRF&Ms are illustrated in blue and red, respectively. The results are presented as the mean ± 1 SD (shaded area).

0.79 to 0.98, median 0.93) and resultant JRFs (r ranging from 0.78 to 0.99, median 0.97). The variables showing the largest discrepancies between the two datasets were transverse GRM (r ranging from -0.19 to 0.86, median 0.09), frontal GRM (r ranging from 0.39 to 0.96, median 0.59) and medio-lateral GRF (r ranging from 0.12 to 0.96, median 0.61). The model consistently overestimated the computed peak forces with the only clear exceptions being the resultant JRFs for the right leg (RL) during ASP, which were consistently underestimated, the ankle peak resultant JRF during side-cut, and peak vertical GRFs for the RL and left leg (LL) during ASP, which showed similar values. The Wilcoxon-paired sample tests showed significant differences for all peak forces, except ankle peak resultant JRF during side-cut ($p = 0.64$) and peak vertical GRF for the RL ($p = 0.10$) and LL ($p = 0.07$) during ASP. The results for each movement are summarized in the following.
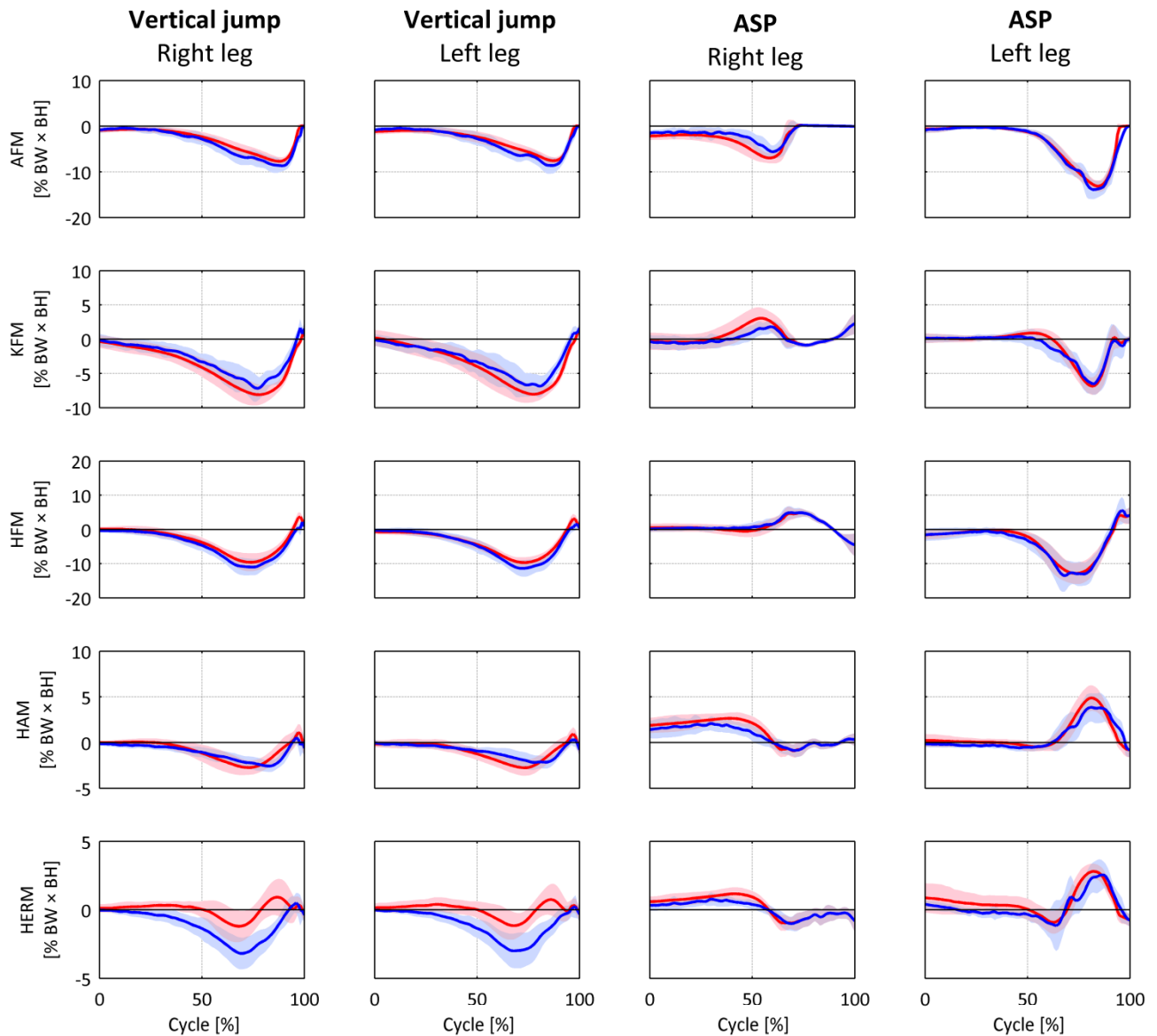
Figure 6 (b) – Results for vertical jump and accelerate from standing position (ASP), illustrating ankle (AFM), knee (KFM) and hip flexion moment (HFM), hip abduction moment (HAM) and hip external rotation moment (HERM). The variables associated with the predicted and measured GRF&Ms are illustrated in blue and red, respectively. The results are presented as the mean ± 1 SD (shaded area).

3.1 Running

For the GRF&Ms during running, strong to excellent correlations were observed for all variables of notable magnitude, including vertical GRF (0.99 ± 0.01), antero-posterior GRF (0.88 ± 0.12), and sagittal GRM (0.87 ± 0.09), whereas the forces and moments of relatively small magnitude showed weak to moderate correlations, specifically medio-lateral GRF (0.12 ± 0.38), frontal GRM (0.50 ± 0.24) and transverse GRM (-0.04 ± 0.33). Overall, the model provided comparable estimates of joint kinetics, showing strong to excellent correlations for all joint moments (r ranging from 0.71 to 0.92) and resultant JRFs (r ranging from
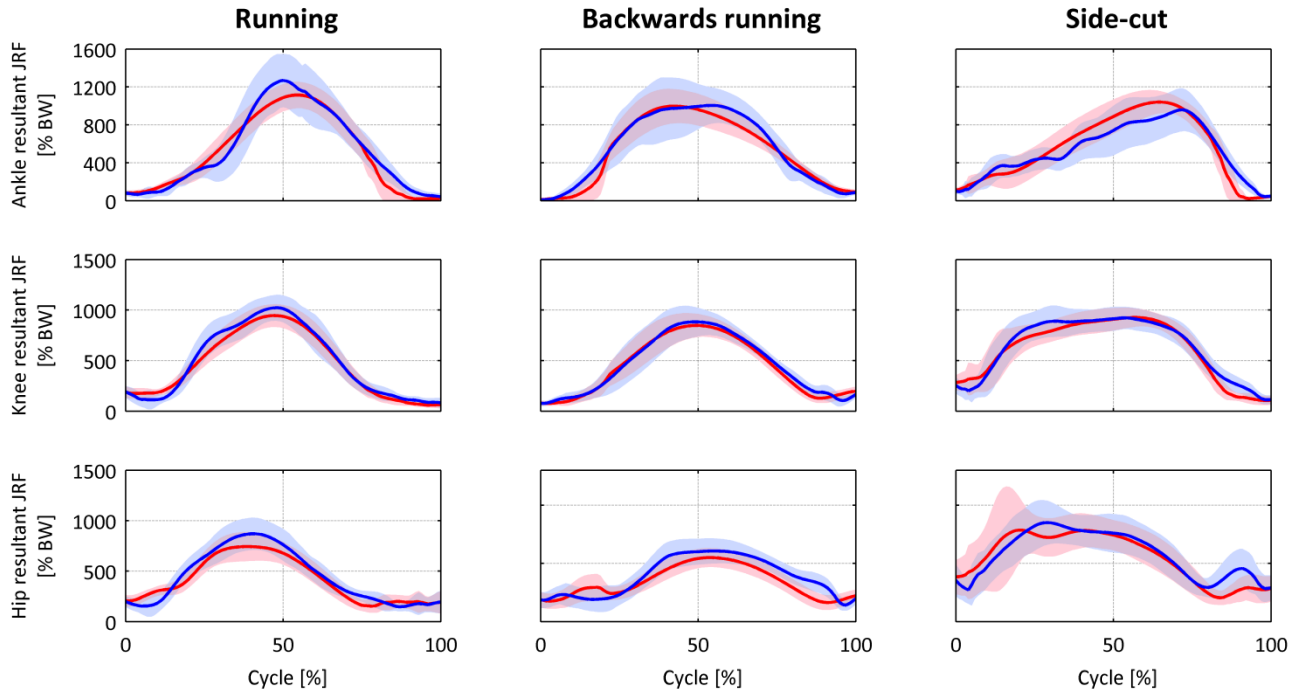
Figure 7 (a) – Results for running, backwards running and side-cut, illustrating the ankle, knee and hip resultant JRFs. The variables associated with the predicted and measured GRF&Ms are illustrated in blue and red, respectively. The results are presented as the mean ± 1 SD (shaded area).

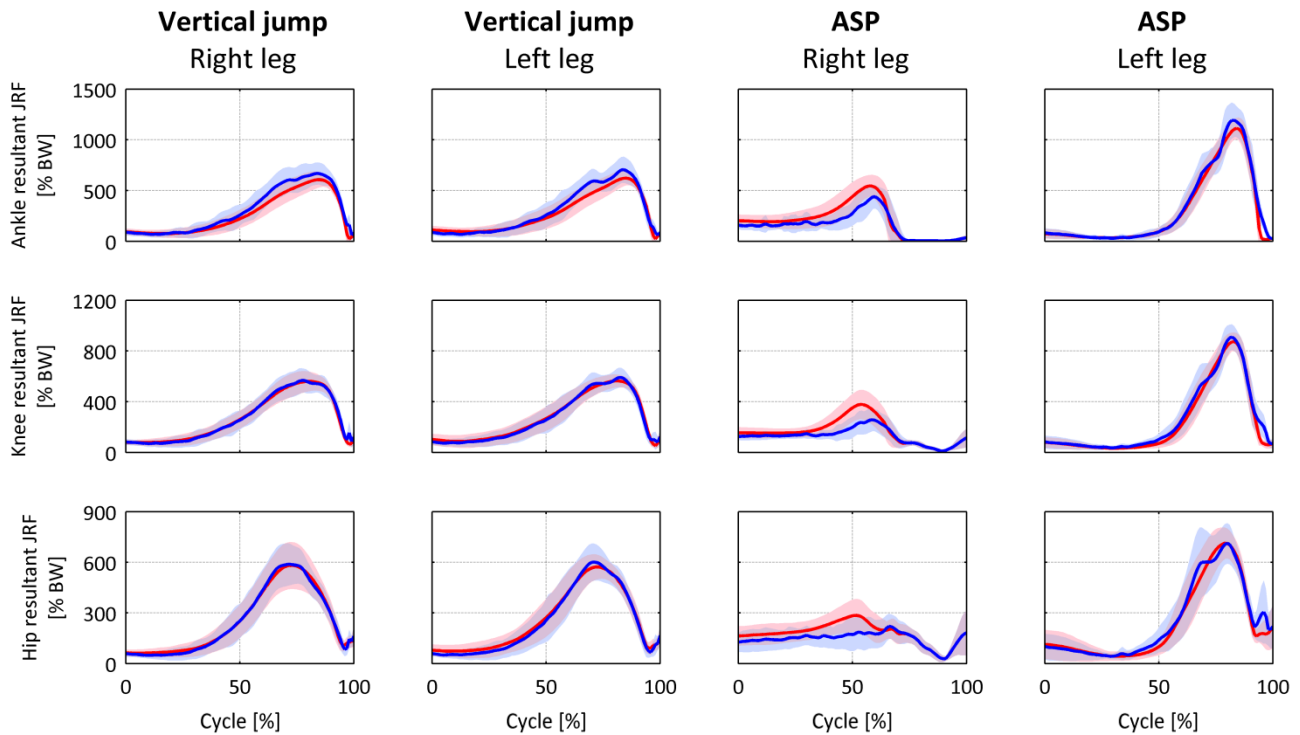**Figure 7 (b) – Results for vertical jump and accelerate from standing position (ASP), illustrating the ankle, knee and hip resultant JRFs. The variables associated with the predicted and measured GRF&Ms are illustrated in blue and red, respectively. The results are presented as the mean ± 1 SD (shaded area).**

Table 1 (a) – RMSD for the selected variables during running, backwards running and side-cut. The results are presented as the mean ± 1 SD.

Variable	Running	Backwards running	Side-cut
Anterior-posterior GRF (N/kg)	7.86 ± 3.55	6.73 ± 1.37	13.04 ± 4.02
Medio-lateral GRF (N/kg)	5.61 ± 1.48	4.62 ± 1.27	8.56 ± 1.60
Vertical GRF (N/kg)	15.66 ± 3.49	12.59 ± 3.57	17.11 ± 4.08
Frontal GRM (Nm/kg)	1.75 ± 0.43	1.61 ± 0.43	1.65 ± 0.50
Sagittal GRM (Nm/kg)	3.60 ± 1.50	2.95 ± 1.00	3.46 ± 0.95
Transverse GRM (Nm/kg)	1.17 ± 0.32	0.90 ± 0.32	2.75 ± 0.52
AFM (Nm/kg)	3.31 ± 1.15	2.57 ± 1.01	1.03 ± 0.27
KFM (Nm/kg)	2.14 ± 0.56	1.55 ± 0.56	2.36 ± 1.45
HFM (Nm/kg)	2.73 ± 0.87	2.20 ± 0.51	3.52 ± 2.05
HAM (Nm/kg)	1.50 ± 0.44	1.36 ± 0.43	2.82 ± 0.79
HERM (Nm/kg)	1.19 ± 0.32	0.88 ± 0.32	2.77 ± 0.70
Ankle resultant JRF (N/kg)	177.54 ± 62.88	147.40 ± 55.78	172.62 ± 53.52
Knee resultant JRF (N/kg)	75.49 ± 22.62	61.22 ± 14.68	88.82 ± 30.45
Hip resultant JRF (N/kg)	99.56 ± 24.16	97.38 ± 20.97	131.91 ± 75.01

Table 1 (b) – RMSD for the selected variables during vertical jump and ASP. The results are presented as the mean ± 1 SD.

Variable	Vertical jump Right leg	Vertical jump Left leg	ASP Right leg	ASP Left leg
Anterior-posterior GRF (N/kg)	4.58 ± 1.61	4.45 ± 1.52	3.44 ± 1.24	3.93 ± 1.17
Medio-lateral GRF (N/kg)	2.16 ± 0.61	2.06 ± 0.54	1.89 ± 0.74	2.97 ± 1.12
Vertical GRF (N/kg)	6.93 ± 1.36	7.07 ± 2.10	6.97 ± 2.18	9.65 ± 1.92
Frontal GRM (Nm/kg)	1.32 ± 0.28	1.27 ± 0.35	0.51 ± 0.19	0.93 ± 0.13
Sagittal GRM (Nm/kg)	0.50 ± 0.19	0.61 ± 0.22	1.76 ± 0.38	1.15 ± 0.24
Transverse GRM (Nm/kg)	0.93 ± 0.35	1.07 ± 0.39	0.56 ± 0.17	0.94 ± 0.19
AFM (Nm/kg)	1.06 ± 1.53	1.03 ± 0.27	1.35 ± 0.29	1.11 ± 0.31
KFM (Nm/kg)	1.23 ± 0.29	1.23 ± 0.23	0.91 ± 0.32	1.00 ± 0.30
HFM (Nm/kg)	1.28 ± 0.42	1.30 ± 0.36	0.96 ± 0.44	1.45 ± 0.54
HAM (Nm/kg)	0.73 ± 0.18	0.70 ± 0.17	0.72 ± 0.33	0.87 ± 0.30
HERM (Nm/kg)	1.54 ± 0.70	1.45 ± 0.65	0.40 ± 0.18	0.95 ± 0.53
Ankle resultant JRF (N/kg)	70.73 ± 17.75	72.55 ± 18.81	92.93 ± 21.83	74.17 ± 24.11
Knee resultant JRF (N/kg)	32.82 ± 5.68	34.75 ± 11.83	67.30 ± 24.12	49.04 ± 13.89
Hip resultant JRF (N/kg)	35.62 ± 10.39	37.98 ± 14.55	57.08 ± 18.40	57.87 ± 22.70

Table 2 (a) - Pearson's correlation coefficients for the selected variables during running, backwards running and side-cut. The results are presented as the mean ± 1 SD.

Variable	Running	Backwards running	Side-cut
Anterior-posterior GRF	0.88 ± 0.12	0.94 ± 0.02	0.89 ± 0.13
Medio-lateral GRF	0.12 ± 0.38	0.53 ± 0.27	0.96 ± 0.02
Vertical GRF	0.99 ± 0.01	0.99 ± 0.00	0.96 ± 0.02
Frontal GRM	0.50 ± 0.24	0.39 ± 0.34	0.59 ± 0.30
Sagittal GRM	0.87 ± 0.09	0.88 ± 0.09	0.79 ± 0.09
Transverse GRM	-0.04 ± 0.33	0.09 ± 0.34	0.86 ± 0.09
AFM	0.89 ± 0.07	0.89 ± 0.09	0.79 ± 0.10
KFM	0.92 ± 0.05	0.94 ± 0.05	0.94 ± 0.10
HFM	0.85 ± 0.05	0.88 ± 0.06	0.92 ± 0.06
HAM	0.90 ± 0.10	0.85 ± 0.13	0.35 ± 0.36
HERM	0.71 ± 0.21	0.68 ± 0.31	0.60 ± 0.22
Ankle resultant JRF	0.93 ± 0.04	0.93 ± 0.05	0.88 ± 0.12
Knee resultant JRF	0.98 ± 0.01	0.98 ± 0.01	0.95 ± 0.04
Hip resultant JRF	0.94 ± 0.05	0.85 ± 0.14	0.83 ± 0.14

Table 2 (b) - Pearson's correlation coefficients for the selected variables during vertical jump and ASP. The results are presented as the mean ± 1 SD.

Variable	Vertical jump Right leg	Vertical jump Left leg	ASP Right leg	ASP Left leg
Anterior-posterior GRF	0.63 ± 0.28	0.68 ± 0.25	0.97 ± 0.02	0.99 ± 0.01
Medio-lateral GRF	0.83 ± 0.13	0.86 ± 0.08	0.61 ± 0.27	0.59 ± 0.37
Vertical GRF	0.98 ± 0.01	0.98 ± 0.01	0.99 ± 0.01	0.99 ± 0.01
Frontal GRM	0.96 ± 0.02	0.96 ± 0.02	0.83 ± 0.12	0.47 ± 0.37
Sagittal GRM	0.92 ± 0.08	0.87 ± 0.12	0.69 ± 0.13	0.95 ± 0.03
Transverse GRM	-0.13 ± 0.39	-0.19 ± 0.47	0.78 ± 0.17	0.60 ± 0.27
AFM	0.96 ± 0.02	0.96 ± 0.02	0.89 ± 0.07	0.98 ± 0.01
KFM	0.95 ± 0.03	0.95 ± 0.03	0.86 ± 0.08	0.92 ± 0.06
HFM	0.98 ± 0.01	0.98 ± 0.01	0.93 ± 0.06	0.97 ± 0.02
HAM	0.78 ± 0.19	0.72 ± 0.26	0.92 ± 0.06	0.87 ± 0.10
HERM	0.50 ± 0.39	0.55 ± 0.34	0.93 ± 0.05	0.77 ± 0.14
Ankle resultant JRF	0.97 ± 0.01	0.97 ± 0.01	0.91 ± 0.06	0.98 ± 0.01
Knee resultant JRF	0.99 ± 0.01	0.99 ± 0.01	0.88 ± 0.07	0.99 ± 0.01
Hip resultant JRF	0.99 ± 0.01	0.99 ± 0.00	0.78 ± 0.14	0.97 ± 0.04

Table 3 (a) – Results of the Wilcoxon paired-sample tests for running, backwards running and side-cut, listing the mean difference ± 1 SD between peak forces. Significant difference is indicated with a *.

Variable (N/kg)	Running	Backwards running	Side-cut
Peak vertical GRF	-13.44 ± 7.00*	-13.48 ± 9.04*	-13.64 ± 8.59*
Ankle peak resultant JRF	-269.80 ± 203.44*	-153.68 ± 137.08*	11.15 ± 143.02
Knee peak resultant JRF	-110.25 ± 66.03*	-54.18 ± 54.08*	-34.08 ± 113.36*
Hip peak resultant JRF	-142.03 ± 68.80*	-84.26 ± 56.73*	1.78 ± 294.93*

Table 3 (b) – Results of the Wilcoxon paired-sample tests for vertical jump and ASP, listing the mean difference ± 1 SD between peak forces. Significant difference is indicated with a *.

Variable (N/kg)	Vertical jump Right leg	Vertical jump Left leg	ASP Right leg	ASP Left leg
Peak vertical GRF	-6.45 ± 5.15*	-7.58 ± 8.13*	1.42 ± 4.27	-3.14 ± 9.27
Ankle peak resultant JRF	-128.52 ± 66.94*	-125.14 ± 81.32*	68.55 ± 63.56*	-146.14 ± 110.16*
Knee peak resultant JRF	-35.36 ± 39.01*	-47.89 ± 39.58*	90.56 ± 64.93*	-42.56 ± 50.52*
Hip peak resultant JRF	-23.20 ± 47.07*	-39.91 ± 51.68*	25.16 ± 51.70*	-52.96 ± 77.04*

0.93 to 0.99). However, significant differences were found for all peak forces with the mean difference ranging from -13.44 ± 7.00 (peak vertical GRF) up to -269.80 ± 203.44 N/kg (ankle peak resultant JRF).

3.2 Backwards running

Similar to running, the results for backwards running showed strong to excellent correlations for vertical GRF (0.99 ± 0.00), antero-posterior GRF (0.94 ± 0.02), and sagittal GRM (0.88 ± 0.09), whereas weak to moderate correlations were found for medio-lateral GRF (0.53 ± 0.27), frontal GRM (0.39 ± 0.34), and transverse GRM (0.09 ± 0.34). Furthermore, strong to excellent correlations were found for all joint moments (*r* ranging from 0.68 to 0.94) and resultant JRFs (*r* ranging from 0.85 to 0.98). Significant differences were found for all peak forces with the mean difference ranging from -13.48 ± 9.04 (peak vertical GRF) up to -153.68 ± 137.08 N/kg (ankle peak resultant JRF).

3.3 Side-cut

Compared to the two running activities, the medio-lateral GRF and transverse GRM were of considerably higher magnitude during side-cut, resulting in correlation coefficients of 0.96 ± 0.02 and 0.86 ± 0.09, respectively. Otherwise, similar results were found for vertical GRF (0.96 ± 0.02), antero-posterior GRF (0.89 ± 0.13), frontal (0.59 ± 0.30) and sagittal GRM (0.79 ± 0.09). Joint flexion moments (*r* ranging from 0.79 to 0.94) and resultant JRFs (*r* ranging from 0.83 to 0.95) showed strong to excellent correlations, whereas

HAM (0.35 ± 0.36) and HERM (0.60 ± 0.22) showed a weak and moderate correlation, respectively. Significant differences were found for all peak forces, except ankle peak resultant JRF (mean diff. = 11.15 ± 143.02 N/kg).

3.4 Vertical jump

For vertical jump, the majority of the variables showed comparable results between datasets, and similar results for the RL and LL, highlighted by the strong to excellent correlations found for vertical GRF (0.98 ± 0.01), frontal GRM (0.96 ± 0.02), sagittal GRM (RL: 0.92 ± 0.08, LL: 0.87 ± 0.12), joint flexion moments (r ranging from 0.95 to 0.98, median 0.96) and resultant JRFs (r ranging from 0.97 to 0.99, median 0.99). Weak to strong correlations were found for the remaining variables (r ranging from -0.13 to 0.78, median 0.59), for which, however, the forces and moments were of considerably lower magnitude. Significant differences were found for all peak forces with the mean difference ranging from -6.45 ± 5.15 (RL peak vertical GRF) to 128.52 ± 66.94 N/kg (RL ankle peak resultant JRF).

3.5 ASP

Compared to vertical jump, ASP involved different movement patterns for each leg, leading to different characteristics in the resulting kinetic data. However, the statistical results were similar between legs for the majority of the variables with the main findings being the excellent correlations for vertical GRF (0.99 ± 0.01) and antero-posterior GRF (RL: 0.97 ± 0.02, LL: 0.99 ± 0.01), and the strong to excellent correlations found for all joint moments (r ranging from 0.77 to 0.98, median 0.92) and resultant JRFs (r ranging from 0.78 to 0.99, median 0.94). The most notable differences between the variables associated with each leg were the frontal (RL: 0.83 ± 0.12, LL: 0.47 ± 0.37) and sagittal GRM (RL: 0.69 ± 0.13, LL: 0.95 ± 0.03). Significant differences were found for all peak forces, except peak vertical GRF for both the RL (mean diff. = 1.42 ± 4.27 N/kg) and LL (mean diff. = -3.14 ± 9.27 N/kg).

4. Discussion

In this study, the method of Fluit et al. (2014a) was adopted and validated for an array of movements associated with sports, using kinematic data and a scaled musculoskeletal model only to predict GRF&Ms. Alterations were made in an attempt to improve the original method, which included the implementation of a new smoothing function and additional contact points to the dynamic contact model. The predicted GRF&Ms and associated joint kinetics were compared to the corresponding variables from a model applying a traditional IDA approach in the AMS, in which the GRF&Ms were measured using force plates.

Across all movements, the majority of the variables showed comparable results between datasets. The main findings were that the model was able to provide estimates comparable to the traditional IDA approach for vertical GRF, joint flexion moments and resultant JRFs. These results were, furthermore, overall similar between movements involving only single support (e.g. running), entirely double support (vertical jump) and a transition from double to single support (ASP). As described by Fluit et al. (2014a), increased errors in the model estimates can be expected when the external forces and moments need to be distributed over both feet. In the present study, however, the results for vertical jump surprisingly showed the highest overall correlations for joint flexion moments and resultant JRFs. The results for the GRMs, antero-posterior and medio-lateral GRFs varied between movements and discrepancies were identified, particularly for the transverse and frontal GRMs. However, the discrepancies were generally associated with variables of low magnitude and could be contributed to the influence of noise on the correlations. The transverse GRMs showed the lowest correlations between datasets, which was consistent with the findings of Fluit et al. (2014a). This result could be partly caused by the constraint imposed by the simplified model of the knee as a hinge-joint, which did not allow for transversal rotation. This issue could, furthermore, have caused the relatively poor agreement of the HERM for the majority of the movements. Finally, despite the overall similarities in the datasets, the computed peak vertical GRFs and resultant JRFs showed discrepancies and significant differences were established for the majority of these variables.

Previous studies in this area have applied their methods for predicting GRF&Ms to the analysis of gait (Fluit et al., 2014a; Eel Oh et al., 2013; Ren et al., 2008), simple static postures, such as stance (Choi et al., 2013; Audu et al., 2007), or activities of daily living, such as deep squatting and stair ascent (Fluit et al., 2014a). This paper presented, for the first time, the prediction of GRF&Ms during movements that are widely used in sports and recreational exercise, involving considerably higher segment accelerations and force magnitudes compared to previous studies. It was expected that the larger accelerations in particular could lead to inaccuracies in the kinetic measures due to the increased importance of the inertial and mass properties of the segments. Furthermore, the higher accelerations are likely to increase errors in the kinematic data, especially due to the larger deformations of soft tissues. However, these issues did not appear to have a critical effect on the kinetic measures in the present study, as overall comparable results were obtained for both the predicted GRF&Ms and the joint kinetics.

As mentioned above, the discrepancies found for the medio-lateral GRFs, frontal and transverse GRMs could be largely contributed to the low magnitude of these variables, which increased the influence of noise. When these variables increased in magnitude, the correlations between datasets likewise increased, such as the frontal GRMs during vertical jump ($r = 0.96 \pm 0.02$) and transverse GRM during side-

cut (r = 0.86 ± 0.09). This tendency indicates that noise was the predominant issue for these inaccuracies. Furthermore, variables displaying such low magnitudes would presumably not be of primary interest for most studies and the lower accuracy of these estimates could, therefore, be of minor importance.

A number of limitations should be noted. First, it is well-known that marker trajectories are associated with noise, especially due to soft-tissue artefacts (Cappozzo et al., 2005), and methods to sufficiently compensate for these inaccuracies does currently not exist (Benoit et al., 2015). Second, the foot was modelled as a single segment and the dynamic contact model could have been improved by applying a multi-segment foot model. In particular, a model that enables bending of the toes, hereby increasing the foot-ground contact surface during toe-off. Third, the muscle models did not incorporate excitation-contraction dynamics, which might have altered the predicted GRF&Ms, as the activation level of the muscle-like actuators were solved as part of the muscle recruitment. Finally, the study could benefit from a comprehensive sensitivity analysis, thus determining the influence of multiple parameters associated with the dynamic contact model.

In order to improve the model's prediction of GRF&Ms, a number of parameters could be adjusted in the dynamic contact model. First, the contact point offsets were approximated, considering the sole thickness of the running shoes and the soft tissue under the heel, and measurements of these parameters could possibly improve the ground contact determination. However, the points are required to overlap with the artificial ground plane in the model environment and have to be adjusted accordingly. Second, the number and position of the contact points could be adjusted to provide more detailed modelling of the foot-ground contact, accounting for the underside characteristics of the foot or specific footwear used. Third, a sensitivity analysis could have been performed on the contact parameters, F_{max}, z_{limit}, and v_{limit}, as well as the threshold values for z_{ratio} and v_{ratio}, hereby determining a set of optimal values. This could potentially have reduced the consistent overestimations of peak forces that were identified for nearly all movements and represented the clearest discrepancy between datasets. Therefore, a comprehensive sensitivity analysis involving all or several of the contact parameters should be deployed to find an optimal combination, aimed towards achieving the highest possible accuracy in the model estimates.

The presented method predominately showed comparable results to traditional IDA, providing a number of valuable opportunities for future studies, particularly within sports science research. By obviating the need for force plate measurements, this method facilitates the analysis of sports-related movements that occupy a large space or can only be analysed in their entirety in outdoor environments. Furthermore, the method excludes the potential influence of force plate targeting, which was implemented during the side-cut manoeuvre for instance. Another potential benefit of this method is that it enables the

determination of GRF&Ms in situations, where force plates are difficult and expensive to instrument, such as motion analysis during treadmill walking or running. In addition, it can be combined with motion analysis systems that do not commonly incorporate an interface between kinematic and force plate data, for example, electromagnetic tracking systems (Frantz et al., 2003) or a combination of miniature gyroscopes and accelerometers (Luinge and Veltink, 2005). Finally, an exciting perspective is the combination of the method with marker-less motion capture systems, as for instance the method presented in Sandau et al. (2014), or incorporating the method in prospective simulations (Fluit et al. 2014b). Recently, Skals et al. (2014) introduced an interface between marker-less motion capture data and a musculoskeletal model, incorporating the method for predicting GRF&Ms of Fluit et al. (2014a), thus providing the first step towards complete IDA using such systems. Therefore, future studies should continue exploring new and improved approaches for marker-less motion analysis to obtain a sufficient level of accuracy as well as continually improve methods for predicting GRF&Ms, particularly focusing on models for accurate ground contact determination.

5. Conclusion

Prediction of GRF&Ms can reduce dynamic inconsistency and obviate the need for force plate measurements when performing IDA on musculoskeletal models. This study provided validation of a method to predict GRF&Ms from full-body motion only for an array of sports-related movements. The method provided estimates comparable to traditional IDA for the majority of the analysed variables, including vertical GRF, joint flexion moments and resultant JRFs. Based on these results, the method could be used instead of force plate data when performing IDA, hereby facilitating the analysis of sports-related movements and providing new opportunities for complete IDA using systems that does not provide and interface between kinematic and force plate data.

6. References

Andersen, M. S., Damsgaard, M., MacWilliams, B. & Rasmussen, J. 2010, "A computationally efficient optimisation-based method for parameter identification of kinematically determinate and over-determinate biomechanical systems", *Comput. Methods Biomech. Biomed. Engin.,* vol. 13, no. 2, pp. 171–183.

Andersen, M. S., Damsgaard, M. & Rasmussen, J. 2009, "Kinematic analysis of over-determinate biomechanical systems", *Comput. Methods Biomech. Biomed. Engin.*, vol. 12, no. 4, pp. 371–384.

Anderson, F. C. & Pandy, M. G. 2001, "Dynamic optimization of human walking", *J. Biomech. Eng.*, vol. 123, no. 5, pp. 381-190.

The AnyBody Modeling System (Version 6.05) (2015). [Computer software]. Aalborg, Denmark: AnyBody Technology. Available from http://www.anybodytech.com

Audu, M. L., Kirsch, R. F. & Triolo, R. J. 2007, "Experimental verification of a computational technique for determining ground reactions in human bipedal stance", *J. Biomech*., vol. 40, no. 5, pp. 1115–1124.

Audu, M. L., Kirsch, R. F. & Triolo, R. J. 2003, "A computational technique for determining the ground reaction forces in human bipedal stance", *J. Appl. Biomech.*, vol. 19, no. 4, pp. 361–371.

Barret, R. S., Besier, T. F. & Lloyd, D. G. 2007, "Individual muscle contributions to the swing phase of gait: An EMG-based forward dynamics modelling approach", *Simul. Model. Pract. Th.*, vol. 15, no. 9, pp. 1146-1155.

Benoit, D. L., Damsgaard, M. & Andersen, M. S. 2015, "Surface marker cluster translation, rotation, scaling and deformation: Their contribution to soft tissue artefact and impact on knee joint kinematics", *J. Biomech.*, Available online 27 March 2015, http://dx.doi.org/10.1016/j.jbiomech.2015.02.050.

Cahouët, V., Luc, M. & David, A. 2002, "Static optimal estimation of joint accelerations for inverse dynamics problem solution", *J. Biomech.*, vol. 35, no. 11, pp. 1507–1513.

Cappozzo, A., Della Croce, U., Leardini, A. & Chiari, L. 2005, "Human movement analysis using stereophotogrammetry. Part 1: theoretical background", *Gait Posture*, vol. 21, no. 2, pp. 186–196.

Carbone, V., Fluit, R., Pellikaan, P., van der Krogt, M. M., Jansen, D., Damsgaard, M., Vigneron, L., Feilkas, T., Koopman, H. F. J. M., Verdonschot, N. 2015, "TLEM 2.0 - A comprehensive musculoskeletal geometry dataset for subject-specific modeling of lower extremity", *J. Biomech.*, vol. 48, no. 5, pp. 734-741.

Challis, J. H. 2001, "The variability in running gait caused by force plate targeting", *J. Appl. Biomech.*, vol. 17, no. 1, pp. 77–83.

Chiari, L., Croce, U. D., Leardini, A. & Cappozzo, A. 2005, "Human movement analysis using stereophotogrammetry. Part 2: Instrumental errors", *Gait Posture*, vol. 21, no. 2, pp. 197–211.

Choi, A., Lee, J.-M. & Mun, J. H. 2013, "Ground reaction forces predicted by using artificial neural network during asymmetric movements", *Int. J. Precis. Eng. Manuf.*, vol. 14, no. 3, pp. 475–483.

Clauser, C. E., McConville, J. T. & Young, J. W. 1969, "Weight, volume, and center of mass of segments of the human body", DTIC Document.

Collins, S. H., Adamczyk, P. G., Ferris, D. P. & Kuo, A. D. 2009, "A simple method for calibrating force plates and force treadmills using an instrumented pole", *Gait Posture*, vol. 29, no. 1, pp. 59-64.

Damsgaard, M., Rasmussen, J., Christensen, S. T., Surma, E. & de Zee, M. 2006, "Analysis of musculoskeletal systems in the AnyBody Modeling System", *Simul. Model. Pract. Theory*, vol. 14, no. 8, pp. 1100–1111.

Della Croce, U., Leardini, A., Chiari, L. & Cappozzo, A. 2005, "Human movement analysis using stereophotogrammetry. Part 4: assessment of anatomical landmark misplacement and its effects on joint kinematics", *Gait Posture*, vol. 21, no. 2, pp. 226–237.

Delp, S. L., Anderson, F. C., Arnold, A. S., Loan, P., Habib, A., John, C. T., Guendelman, E. & Thelen, D. G. 2007, "OpenSim: Open-Source Software to Create and Analyze Dynamic Simulations of Movement", *IEEE Trans. Biomed. Eng.*, vol. 54, no. 11, pp. 1940–1950.

Eel Oh, S., Choi, A. & Mun, J. H. 2013, "Prediction of ground reaction forces during gait based on kinematics and a neural network model", *J. Biomech.*, vol. 46, no. 14, pp. 2372–2380.

Erdemir, A., McLean, S. & Herzog, W. 2007, "Model-Based Estimation of Muscle Forces Exerted during Movements", *Clin. Biomech.*, vol. 22, no. 2, pp. 131-154.

Fluit, R., Andersen, M. S., Kolk, S., Verdonschot, N. & Koopman, H. F. J. M. 2014a, "Prediction of ground reaction forces and moments during various activities of daily living", *J. Biomech.*, vol. 47, no. 10, pp. 2321–2329.

Fluit, R., Andersen, M. S., Verdonschot, N., Koopman, H. F. J. M. 2014b, "Optimal inverse dynamic simulation of human gait", *Gait Posture*, vol. 39, Supplement 1, pp. S42.

Frantz, D. D., Wiles, A. D., Leis, S. E. & Kirsch, S. R. 2003, "Accuracy assessment protocols for electromagnetic tracking systems", *Phys. Med. Biol.*, vol. 48, no. 14, pp. 2241-2251.

Hatze, H. 2002, "The fundamental problem of myoskeletal inverse dynamics and its implications", *J. Biomech.*, vol. 35, no. 1, pp. 109–115.

Horsman, M. D. K., Koopman, H. F. J. M., van der Helm, F. C. T., Prosé, L. P., Veeger, H. E. J. 2007, "Morphological muscle and joint parameters for musculoskeletal modelling of the lower extremity", *Clin. Biomech.*, vol. 22, no. 2, pp. 239–247.

Kuo, A. D. 1998, "A least-squares estimation approach to improving the precision of inverse dynamics computations", *J. Biomech. Eng.*, vol. 120, no. 1, pp. 148-159.

Leardini, A., Chiari, L., Croce, U. D. & Cappozzo, A. 2005, "Human movement analysis using stereophotogrammetry. Part 3. Soft tissue artifact assessment and compensation", *Gait Posture*, vol. 21, no. 2, pp. 212–225.

Luinge, H. J. & Veltink, P. H. 2005, "Measuring orientation of human body segments using miniature gyroscopes and accelerometers", *Med. Biol. Eng. Comput.*, vol. 43, no. 2, pp. 273–282.

Lund, M. E., Andersen, M. S., de Zee, M. & Rasmussen, J. 2015, "Scaling of musculoskeletal models from static and dynamic trials", *Int. Biomech.*, vol. 2, no. 1, pp. 1–11.

Mellon, S. J., Grammatopoulos, G., Andersen, M. S., Pegg, E. C., Pandit, H. G., Murray, D. W. & Gill, H. S. 2013, "Individual motion patterns during gait and sit-to-stand contribute to edge-loading risk in metal-on-metal hip resurfacing", *Proc. Inst. Mech. Eng. H J. Eng. Med.*, vol. 227, no. 7, pp. 799-810.

Mellon, S. J., Grammatopoulos, G., Andersen, M. S., Pandit, H. G., Gill, H. S. & Murray, D. W. 2015, "Optimal acetabular component orientation estimated using edge-loading and impingement risk in patients with metal-on-metal hip resurfacing arthroplasty", *J. Biomech*, vol. 48, no. 2, pp. 318-323.

Middleton, J., Sinclair, P. & Patton, R. 1999, "Accuracy of centre of pressure measurement using a piezoelectric force platform", *Clin. Biomech.*, vol. 14, no. 14, pp. 357–360.

Nigg, B. M. 2006. Force. In: NIGG, B. M. & HERZOG, W. (ed.) *Biomechanics of the Musculo-skeletal System, Third Edition*. Chichester, England: John Wiley & Sons Ltd.

Pàmies-Vilà, R., Font-Llagunes, J. M., Cuadrado, J. & Alonso, F. J. 2012, "Analysis of different uncertainties in the inverse dynamic analysis of human gait", *Mech. Mach. Theory*, vol. 58, pp. 153–164.

Payton, C. J. & Bartlett, R. M. 2008, *Biomechanical evaluation of movement in sport and exercise*, Abingdon, United Kingdom: Routledge.

Pearsall, D. J. & Costigan, P. A. 1999, "The effect of segment parameter error on gait analysis results", *Gait Posture*, vol. 9, no. 3, pp. 173–183.

Psycharakis, S. G. & Miller, S. 2006, "Estimation of Errors in Force Platform Data", *Res. Q. Exerc. Sport*, vol. 77, no. 4, pp. 514–518.

Rao, G., Amarantini, D., Berton, E. & Favier, D. 2006, "Influence of body segments' parameters estimation models on inverse dynamics solutions during gait", *J. Biomech.*, vol. 39, no. 8, pp. 1531–1536.

Rasmussen, J., Dahlquist, J., Damsgaard, M., de Zee, M. & Christensen, S. T. 2003a, "Musculoskeletal modeling as an ergonomic design method", in: *Proceedings of the XVth Triennial Congress of the International Ergonomics Association and 7th Joint Conference of the Ergonomics Society of Korea/Japan Ergonomics Society*, Seoul, Korea.

Rasmussen, J., Damsgaard, M., Surma, E., Christensen, S. T., de Zee, M. & Vondrak, V. 2003b, "Anybody - a software system for ergonomic optimization", in: *Fifth World Congress on Structural and Multidisciplinary Optimization*, Venice, Italy.

Rasmussen, J., Damsgaard, M. & Voigt, M. 2001, "Muscle recruitment by the min/max criterion—a comparative numerical study", *J. Biomech.*, vol. 34, no. 3, pp. 409–415.

Ren, L., Jones, R. K. & Howard, D. 2008, "Whole body inverse dynamics over a complete gait cycle based only on measured kinematics", *J. Biomech.*, vol. 41, no. 12, pp. 2750–2759.

Riemer, R. & Hsiao-Wecksler, E. T. 2008, "Improving joint torque calculations: Optimization-based inverse dynamics to reduce the effect of motion errors", *J. Biomech.*, vol. 41, no. 7, pp. 1503–1509.

Riemer, R., Hsiao-Wecksler, E. T. & Zhang, X. 2008, "Uncertainties in inverse dynamics solutions: A comprehensive analysis and an application to gait", *Gait Posture*, vol. 27, no. 4, pp. 578–588.

Robert, T., Causse, J. & Monnier, G. 2013, "Estimation of external contact loads using an inverse dynamics and optimization approach: General method and application to sit-to-stand maneuvers", *J. Biomech.*, vol. 46, no. 13, pp. 2220-2227.

Sandau, M., Koblauch, H., Moeslund, T. B., Aanæs, H., Alkjær, T. & Simonsen, E. B. 2014, "Markerless motion capture can provide reliable 3D gait kinematics in the sagittal and frontal plane", *Med. Eng. Phys.*, vol. 36, no. 9, pp. 1168-1175.

Schwartz, M. H. & Rozumalski, A. 2005, "A new method for estimating joint parameters from motion data", *J. Biomech.*, vol. 38, no. 1, pp. 107-116.

Skals, S. L., Bendtsen, K. M., Rasmussen, K. P. & Andersen, M. S. 2014, "Validation of musculoskeletal models driven by dual Microsoft Kinect Sensor data", in: *13th International Symposium on 3D Analysis of Human Movement*, Lausanne, Switzerland.

Stagni, R., Fantozzi, S., Cappello, A. & Leardini, A. 2005, "Quantification of soft tissue artefact in motion analysis by combining 3D fluoroscopy and stereophotogrammetry: a study on two subjects", *Clin. Biomech.*, vol. 20, no. 3, pp. 320–329.

Taylor, R. 1990, "Interpretation of the correlation coefficient: a basic review", *J. Diagn. Med. Sonog.*, vol. 6, no. 1, pp. 35-39.

Thelen, D. G. & Anderson, F. C. 2006, "Using computed muscle control to generate forward dynamic simulations of human walking from experimental data", *J. Biomech.*, vol. 39, no. 6, pp. 1107-1115.

Van der Helm, F. C. T., Veeger, H. E. J., Pronk, G. M., Van der Woude, L. H. V. & Rozendal, R. H. 1992, "Geometry parameters for musculoskeletal modelling of the shoulder system", *J. Biomech.*, vol. 25, no. 2, pp. 129-144.

Vaughan, C. L., Davis, B. L. & O'Connor, J. C. 1999, *Dynamics of Human Gait, Second Edition*, Western Cape, South Africa: Kiboho Publishers.

Vaughan, C. L., Andrews, J. G. & Hay, J. G. 1982, "Selection of body segment parameters by optimization methods", *J. Biomech. Eng.*, vol. 104, no. 1, pp. 38-44.

Veeger, H. E. J., Van der Helm, F. C. T., Van der Woude, L. H. V., Pronk, G. M. & Rozendal, R. H. 1991, "Inertia and muscle contraction parameters for musculoskeletal modelling of the shoulder mechanism", *J. Biomech.*, vol. 24, no. 7, pp. 615-629.

Weber, T., Al-Munajjed, A. A., Verkerke, G. J., Dendorfer, S. & Renkawitz, T. 2014, "Influence of minimally invasive total hip replacement on hip reaction forces and their orientations", *J. Orthop. Res.*, vol. 32, no. 12, pp. 1680-1687.

Zajac, F. E., Neptune, R. R. & Kautz, S. A. 2003, "Biomechanics and muscle coordination of human walking: part II: lessons from dynamical simulations and clinical implications", *Gait Posture*, vol. 17, no. 1, pp. 1–17.

de Zee, M., Hansen, L., Wong, C., Rasmussen, J. & Simonsen, E. B. 2007, "A generic detailed rigid-body lumbar spine model", *J. Biomech.*, vol. 40, no. 6, pp. 1219-1227.

Appendix

Label	Position	A-P	M-L	P-D
RTHI	Right thigh	Opt.	Opt.	Opt.
LTHI	Left thigh	Opt.	Opt.	Opt.
RKNE	Right lateral epicondyle	Fix.	Fix.	Fix.
LKNE	Left lateral epicondyle	Fix.	Fix.	Fix.
RPSI	Right posterior superior iliac spine	Fix.	Fix.	Fix.
LPSI	Left posterior superior iliac spine	Fix.	Fix.	Fix.
RASI	Right anterior superior iliac spine	Fix.	Fix.	Fix.
LASI	Left anterior superior iliac spine	Fix.	Fix.	Fix.
RANK	Right lateral malleolus	Fix.	Fix.	Fix.
LANK	Left lateral malleolus	Fix.	Fix.	Fix.
RHEE	Right calcaneus	Fix.	Fix.	Fix.
LHEE	Left calcaneus	Fix.	Fix.	Fix.
RTIB	Right tibia	Opt.	Opt.	Opt.
LTIB	Left tibia	Opt.	Opt.	Opt.
RTOE	Right metatarsus	Fix.	Fix.	Fix.
LTOE	Left metatarsus	Fix.	Fix.	Fix.
RMT5	Right fifth metatarsal	Fix.	Fix.	Fix.
LMT5	Left fifth metatarsal	Fix.	Fix.	Fix.
RELB	Right lateral epicondyle	Fix.	Fix.	Fix.
LELB	Left lateral epicondyle	Fix.	Fix.	Fix.
RWRA	Right wrist bar thumb side	Fix.	Fix.	Fix.
LWRA	Left wrist bar thumb side	Fix.	Fix.	Fix.
RFINL	Right first metacarpal	Fix.	Fix.	Fix.
LFINL	Left first metacarpal	Fix.	Fix.	Fix.
RFINM	Right fifth metacarpal	Fix.	Fix.	Fix.
LFINM	Left fifth metacarpal	Fix.	Fix.	Fix.
RUPA	Right triceps brachii	Opt.	Opt.	Opt.
LUPA	Left triceps brachii	Opt.	Opt.	Opt.
RSHO	Right Acromio-clavicular joint	Fix.	Fix.	Fix.
LSHO	Left Acromio-clavicular joint	Fix.	Fix.	Fix.
STRN	Xiphoid process of the sternum	Opt.	Opt.	Opt.
CLAV	Jugular Notch	Opt.	Opt.	Fix.
C7	7th Cervical Vertebrae	Fix.	Fix.	Fix.
RILC*	Right iliac crest	-	-	-
LILC*	Left iliac crest	-	-	-

*Excluded
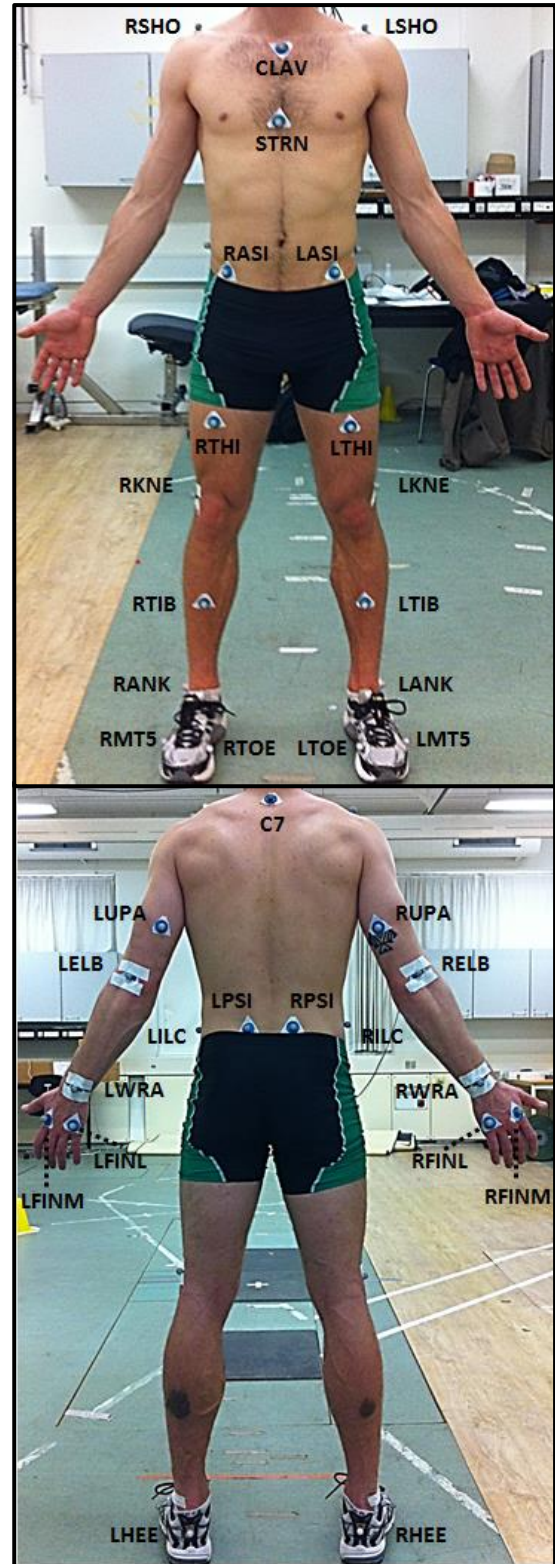
Appendix 1 – Marker protocol, listing marker labels, positions and whether the marker positions were fixed (Fix.) or optimized (Opt.) in the antero-posterior (A-P), medio-lateral (M-L) and proximal-distal (P-D) directions.

Prediction of ground reaction forces and moments during sports-related movements

Worksheets

Sebastian Laigaard Skals

2/6/2015

AALBORG UNIVERSITY

Contents

Theoretical Background

Musculoskeletal modelling has become an inherent part of many areas of research providing insight into the internal forces acting in the body during motion, which are otherwise impractical or impossible to measure. This is accomplished by viewing the human body as a mechanical system consisting of rigid bodies, which enables analysis of the system's behaviour using methods associated with multibody dynamics. Nowadays, several commercial software packages exist that enables detailed and fairly efficient simulation of the musculoskeletal system. This does not mean, however, that computer simulation of the musculoskeletal system is independent from experimental data. On the contrary, these models rely on many different experimental inputs and the quality of these data strongly affects the accuracy of the models' estimation of internal forces. One of these inputs is the external forces acting on the body by the environment, which are measured using various sensors depending on e.g. the task and environment included in the simulation. For studies of human motion, the most commonly measured external forces are the ground reaction forces and moments (GRF&Ms), which are typically obtained using force plates (FP). However, as will become clear in the following, this input can contribute to errors in the model outputs while the dependency on FP measurements imposes practical limitations during motion analysis studies.

In the following, the fundamental information about the procedures associated with the present study is presented by providing an overview of the mechanical analysis of the musculoskeletal system, specifically *Inverse Dynamic Analysis* (IDA). First, the area of musculoskeletal modelling is described, including applications, principles and assumptions, and the overall structure of models. Second, IDA is described in more detail, focusing on the specific approach inherent to the AnyBody Modeling System (AMS) (AnyBody Technology A/S, Aalborg, Denmark) as well as the various experimental inputs to the analysis and associated errors. Finally, limitations of the current approach for IDA are described, focusing on the potential benefits of predicting rather than measuring GRF&Ms.

1. Musculoskeletal modelling

For many years, computer models have been applied to nearly all areas of engineering and are now an indispensable tool to the extent that computer-aided methods have replaced physical experiments for many prototype designs (Lund et al., 2012). The primary benefit associated with creating simulations of the musculoskeletal system is that these models provide estimates of the body's internal behaviour, which are otherwise difficult or impossible to measure experimentally (Zajac and Winthers, 1990). As described by

Pandy (2001), there is a growing belief that musculoskeletal models are able to provide quantitative explanations of how the neuromuscular and musculoskeletal systems interact to produce movement. This belief partly stems from the continuing development of computer systems, which, along with advances in numerical procedures, enables the development and analysis of more comprehensive and, therefore, more realistic models of the musculoskeletal system (Huston, 2001; Pandy, 2001). Today, the application of musculoskeletal models has become more widespread within science and industry due to the availability of modelling software, such as SIMM (Delp and Loan, 1995), OpenSIM (Delp et al., 2007) and the AMS. Musculoskeletal models are now being applied in ergonomic optimization of products and workplaces (Rasmussen et al., 2003a, 2003b), treatment of gait abnormalities (Arnold and Delp, 2005; Zajac et al., 2003), orthopaedics (Mellon et al., 2013, 2015; Weber et al., 2014) and sports biomechanics (Payton and Bartlett, 2008) (Figure 1). Considering these developments, computer simulation could potentially achieve the same significance for studies of the musculoskeletal system as it has for other areas of engineering.

1.1 Objectives and challenges

In general, computer simulation models can be used to 1) increase knowledge and insight about a complex situation and/or 2) estimate how important variables are sensitive to changes in internal or external conditions (Nigg et al., 2006). The mechanical function of the human body is indeed a complex situation. As described by Nigg et al. (2006), the muscles are the active components producing force while bone, cartilage, ligaments and tendons provide various passive functions. The skeletal system can move at joints and the mechanical properties of the joints determine the translational and rotational movement possibilities between body segments. The muscles are activated by the central nervous system (CNS), which chooses a set of muscle actions that enables a desired motion for any position, movement or loading condition (Rasmussen et al., 2001).

From a mechanical point of view, the complexity of the human body partly stems from the geometric and material properties of the system (Huston, 2001). The skeletal structure, muscles and other soft tissues constitute a highly complex geometry and the material properties of the body are irregular, which complicates or prevents the determination of their mechanical function. In addition, two of the main challenges when attempting to describe the dynamics of human motion are the mechanical properties of muscles and the muscle activation pattern. As described by Herzog (2006), many aspects of muscular force production have still not been resolved mainly due to their complicated contractile properties. Likewise, the activation of muscles by the CNS to produce complex movement remains poorly understood (Damsgaard et al., 2006; Manal and Buchanan, 2004). Therefore, computer models need to be simplified and general assumptions about the system's mechanical function are necessary to enable analysis.
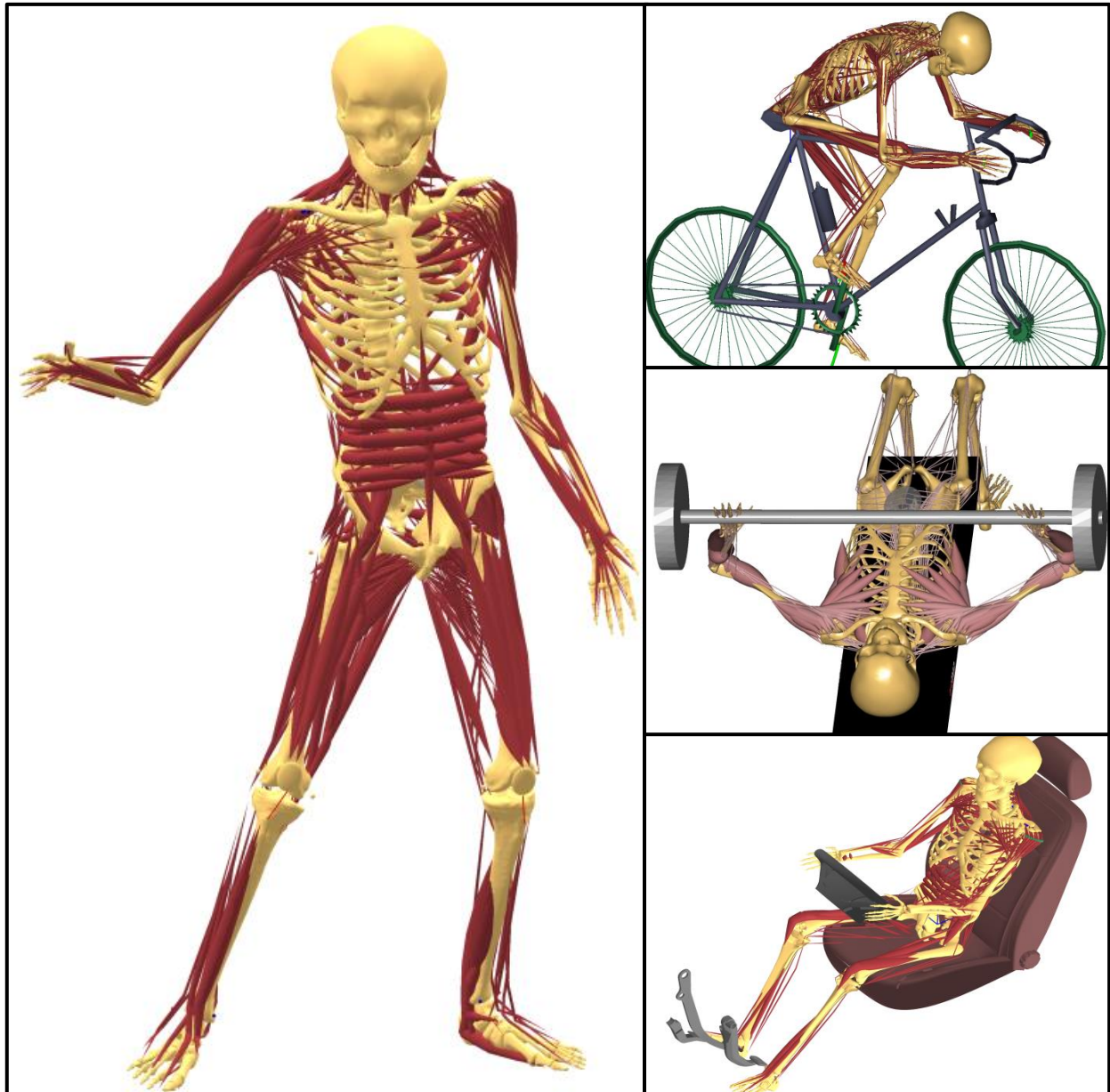
Figure 1 – Musculoskeletal models in the AMS, exemplifying the various applications of models in e.g. sports biomechanics and ergonomics. Courtesy of John Rasmussen.

1.2 Model structure

In musculoskeletal modelling, the body is typically perceived as a multibody mechanical system of rigid bodies, which enables analysis of the system by standard methods of multibody dynamics (Damsgaard et al., 2006). Specifically, the models consist of a series of interconnected segments, representing the arms, legs, torso, neck, and head, i.e., a multibody system simulating the overall frame of the body (Huston, 2001). However, this does not imply a straightforward solution. Multibody mechanical systems exhibit notoriously complex behaviour when driven by internal and/or external forces (Otten, 2003). It is currently infeasible to include all elements and functions of the human body in a musculoskeletal model, but this

does not mean that models cannot provide accurate estimations of the body's mechanical function and, hereby, improve our understanding of the underlying mechanisms of human locomotion.

In general, which elements to include in a musculoskeletal model depends on its intended use and it is generally accepted that the simplest model fulfilling the goal of the research should be deployed (Pandy, 2001; Zajac and Winthers, 1990). This is partly due to the fact that despite the advances in computational resources, musculoskeletal models still need to be highly simplified in order to be reasonably efficient (Damsgaard et al., 2006). As described by Pandy (2001), if the goal of the model is to describe muscle function, the structures contributing to the overall stiffness of the joint are rarely included, such as cartilage, menisci and ligaments. For other applications, however, the contribution of these passive structures might be crucial to obtain accurate simulation results. In a recent example of detailed knee modelling, ligaments were represented as spring elements with nonlinear elastic characteristics (Marra et al., 2015). According to Zajac and Winthers (1990), there are seven major steps that need to be included in a musculoskeletal model to account for multi-muscle control of the body segments during motion. 1) *The body segments and joint kinematics* must be specified. 2) *The dynamical equations of motion* must be derived, which depends on the assumed properties of the joints and interaction between the body segments and the environment. 3) *Passive-joint tissue mechanics* should be modelled unless assumed insignificant, which is often the case as mentioned above. 4) *Geometric joint transformation*, where the joint and musculoskeletal geometry is defined, i.e., the musculoskeletal moment arms relative to the joints' axes of rotations. 5) *The musculotendon force generation process*, which involves the musculotendon structural properties and the dynamical properties of the musculotendon actuator (e.g. muscle excitation-contraction coupling and musculotendon contraction dynamics). 6) *The neuromotor CNS circuitry*, also known as muscle recruitment pattern, which describes how individual muscles are recruited/activated during coordinated movement. 7) *The complete musculoskeletal model* is specified by the interaction between these constituent parts.

1.3 Body segment parameters

Although quite simple models can be adequate for many purposes, it is obvious that more comprehensive and detailed models possess greater potential for providing accurate simulations of the human body. Estimating body segment parameters (BSPs) involves defining the dynamical properties of each body segment by personalising the model to the individual or group it aims to represent (Vaughan et al., 1999). Typically, this can be achieved by measuring total body mass and segment lengths of a subject and applying regression equations to define each segment's mass, centre-of-gravity (COG) and moment-of-inertia (MOI) (Contini et al., 1963). These regression equations are most often derived from cadaver-based studies, which

determine the ratio between e.g. total body mass and segment masses (Clauser et al., 1969). While this information can be used to estimate net torques and forces at the joints, the muscular geometry and other properties, such as muscle insertion points and wrapping surfaces, needs to be reasonably defined if one wishes to determine the force exerted by individual muscles. The geometric definition of the musculoskeletal system will define the moment arms as well as the length of the associated muscles, which, taken together, determines the possible moment that can be produced at the joints by a given muscle force (Horsman et al., 2007). In order to meet these objectives, BSPs are most often determined generally and, subsequently, scaled to the individual or population group the model aims to represent.

The fundamental approach for determining BSPs is cadaver-based studies, such as Clauser et al. (1969) and Carbone et al. (2015). In summary, this procedure involves dissecting a human cadaver and performing various measurements to determine the dimensions, mass, COG and MOI of the severed body segments. Subsequently, regression equations can be formulated based on these descriptive data, which provides estimates of the BSPs in relation to the characteristics of the individual or group of interest. In recent years, these descriptive data have become more detailed. Carbone et al. (2015) and Horsman et al. (2007) used a cadaver-based study to determine additional parameters, as for instance attachment sites of muscles, optimal muscle fibre length and pennation angles. Commonly, the cadaver-based data, providing a more general description of the BSPs and muscular geometry, are combined with subject specific data in order to personalise the model, also referred to as model scaling (Lund et al., 2015). For example, Vaughan et al. (1999) determined BSPs by performing multiple anthropometric measurements to determine the segment dimensions of their subjects and combined this information with regression coefficients obtained through cadaver-based studies. This exemplifies model scaling based on traditional anthropometric measurements, but, in more recent years, scaling has been performed using kinematic data (Lund et al., 2015; Andersen et al., 2010). This approach involves scaling the model based on the position of markers placed at bony landmarks, hence providing an estimate on the skeletal dimensions. Another approach is to perform various scans, such as full body X-ray absorptiometry (Ganley and Powers, 2004), which provides personalised BSP estimates on living subjects. In addition, medical imaging data from living subjects can be used to perform detailed subject-specific scaling. Recently, Carbone et al. (2015) presented the *Twente Lower Extremity Model 2.0*, which is a cadaver-based musculoskeletal model of the lower extremities accompanied by a coherent set of medical imaging data (CT and MRI). The model is freely available and was developed to be easily combined with other imaging data, facilitating detailed subject-specific scaling. Although scanning techniques are considered very accurate, it typically entails high cost and radiation exposure and should be questioned as a routine method (Vaughan et al., 1999).

In the AMS, anthropometric (e.g. Peebles and Norris (1998)) and/or cadaver-based data (e.g. Horsman et al. (2007)) have been used to construct the musculoskeletal models and there are several scaling options, closely corresponding to the different approaches described above. The standard models, based on anthropometric measurements, can be specified to a specific percentile, i.e., the dimensions of the population group of interest. These models can, furthermore, be scaled according to joint-to-joint distances (resembling subject-specific anthropometric measurements), location of bony landmarks (kinematic measurements) and/or subject-specific imaging scans. Another important aspect of scaling is the model's assumed muscle strength. In the AMS, muscle strength is scaled according to the height and mass of the subjects, meaning that a taller and heavier individual will require a lower percentage of total muscle activity to balance a given load compared to a shorter and lighter individual. Additionally, a scaling law can be applied that takes the individual's fat percentage into account. A higher estimated fat percentage will result in less muscle strength, as the volume occupied by muscles is replaced by inactive fat.

1.4 Analytical approaches

While section 1.2 and 1.3 outline the general model structure and personalisation, respectively, there are a number of different analytical approaches to study the biomechanics of human motion. Overall, these approaches are driven by the equations of motion, which provides the relationship between motion and forces in the mechanical system. The equations of motion can be solved in two directions, i.e., by 1) solving the motion from the forces or 2) solving the forces from the motion (Otten, 2003). The approaches mainly associated with 1 include *Forward Dynamics-based tracking methods* (Thelen and Anderson, 2006), *EMG-driven forward dynamics* (Barret et al., 2007), and *Dynamic Optimization* (Anderson and Pandy, 2001). Forward Dynamics-based tracking methods use computed muscle control, employing a feedforward and feedback control, which is held up against measured kinematics to determine the muscle actions that produce the motion (Thelen and Anderson, 2006). EMG-driven forward dynamics involves either identifying the timing of muscle activations from EMG-data to generate a simplified neural input signal (indirect approach) or using the continuous varying time history of the EMG-signal as the neural input to each muscle in the model (direct approach) (Barret et al., 2007). Dynamic Optimization predicts the motor patterns and kinematics of a given motion by solving an optimization problem for the complete movement cycle, implementing a time-dependent performance criterion, i.e., the goal of the motor task (Anderson and Pandy, 2001). The approach mainly associated with 2 is called *Inverse Dynamics* (Erdemir et al., 2007; Damsgaard et al., 2006). IDA applies measurements of body motion and/or external forces as input to the equations of motion to calculate muscle- and joint forces, solving a different optimization problem for each instant during the motion (Pandy, 2001). This inherent feature improves its computational efficiency, which can be exploited to build more complex models, i.e., a finer level of detail and a higher number of muscles

(Damsgaard et al., 2006; Rasmussen et al., 2001). In the present study, the musculoskeletal models are constructed and analysed in the AMS, which exclusively allows for IDA (Damsgaard et al., 2006). Therefore, the specific IDA approach inherent to the AMS will be described in more detail in the following.

2. Inverse dynamics in the AnyBody Modeling System

In general, IDA applies the following input to solve the dynamics of a given motion (Vaughan et al., 1999): 1) BSPs, as described in section 1.3, 2) segment kinematics, i.e., linear- and angular kinematics of body segments, and 3) the external forces acting on the body. If only the BSPs and kinematics are known, the IDA can be completed by iteratively solving the equations of motion for each body segment, using the so-called top-down approach (Riemer and Hsiao-Wecksler, 2008; Cahouët et al., 2002). However, this approach is particularly sensitive to uncertainties in the kinematic data, which can lead to inaccurate joint moment estimations (Cahouët et al., 2002). Alternatively, the bottom-up approach can be used, which includes measurements of the external forces acting on the bottom-most segment, typically the GRF&Ms (Riemer and Hsiao-Wecksler, 2008; Kuo, 1998; Zajac, 1993). When the GRF&Ms are known, they form a boundary condition for the bottom-most segment and dynamic equilibrium is obtained at each successive segment proceeding upwards (Kuo, 1998). By inputting these external forces and moments, the inaccuracies caused by the acceleration inputs can be reduced and the joint moment estimations tends to be more accurate in the bottom part of the multibody system (Riemer and Hsiao-Wecksler, 2008; Zajac, 1993). The improved accuracy of the bottom-up approach is partly due to the fact that external force data is typically less noisy than acceleration data (Kuo, 1998). In the AMS, however, the dynamics of a given motion are not solved iteratively by obtaining equilibrium one segment at a time throughout the kinetic chain. Instead, the muscle and joint forces are calculated by formulating one complete set of dynamic equilibrium equations, whether external forces are included or not (Damsgaard et al., 2006). Solving the dynamic equilibrium equations are, however, preceded by the kinematic analysis, which provides the linear and rotational acceleration of each segment in the model and, together with the boundary conditions, is used to form the equations of motion (Andersen et al., 2009).

2.1 Kinematics

There are multiple methods for performing kinematic analysis that vary greatly in complexity, cost, and accuracy, and the choice of method is typically based on a compromise between these factors. Currently, golden standards for motion analysis include bone-pin studies (Benoit et al., 2006) and 3D fluoroscopy (Stagni et al., 2005), which have very high accuracy. However, bone-pin studies are invasive and 3D fluoroscopy exposes the subject to some degree of radiation while the fluoroscopic field-of-view limits the

analysis to small areas of the body. Another approach is to use wearable inertial motion sensors, such as electromagnetic tracking systems (Frantz et al., 2003) or a combination of miniature gyroscopes and accelerometers (Luinge and Veltink, 2005), which are, however, sensitive to magnetic disturbance and require relatively large data processing units to be fixated on the body, respectively (Fong and Chan, 2010). The most common method for motion analysis is marker-based motion capture, which applies an infrared camera-based system to track the trajectories of reflective skin-markers placed on the body (Figure 2) (Andersen et al., 2009; McGinley et al., 2009; Cappozzo et al., 2005; Manal and Buchanan, 2004; Richards, 1999).

2.1.1 Marker-based motion analysis

There are two camera-based systems for studying human movement, applying either active or passive markers (Manal and Buchanan, 2004). In the present study, a passive-marker system was applied, which is briefly explained in the following based on the descriptions by Manal and Buchanan (2004) and Chiari et al. (2005). Passive markers, or tracking targets, basically reflect projected light, which makes the markers visible to the camera system. In order to reflect more light than surrounding objects, markers are covered in a highly reflective material. A ring of stroboscopic LED's are built into the camera-system to illuminate the markers, enabling each camera to detect markers in their line-of-sight. Subsequently, the 3-D coordinates of each marker can be determined from the multiple 2-D camera views, which are synchronised during an initial calibration procedure. When a marker is visible by multiple cameras, the unique 3-D position of the marker in object-space can be determined as the intersection of rays directed from each camera.

There are multiple approaches for positioning the markers on the body. For gait analysis, for example, many different data acquisition protocols exist, employing different marker-sets and collection procedures as well as underlying biomechanical models (Ferrari et al., 2007). What is common to all marker protocols, however, is that the position of external markers attempt to describe the position of the underlying skeleton (Vaughan et al., 1999). This means that, ideally, markers should be placed at bony landmarks on the body to avoid excessive amounts of soft tissue between the markers and associated skeletal bones. This is also important for repeatability and the determination of joint axes (Cappozzo et al., 2005) as well as predicting internal skeletal landmarks (Vaughan et al., 1999).

As described by Vaughan et al. (1999), six independent coordinates are required to uniquely describe the position of any unconstrained segment in 3-D space, related to the segment's six degrees-of-freedom (DOF). However, the joints connecting individual body segments provide part of the constraints to the motion and it is only the remaining unknowns, or DOF, that are resolved from the motion input data.
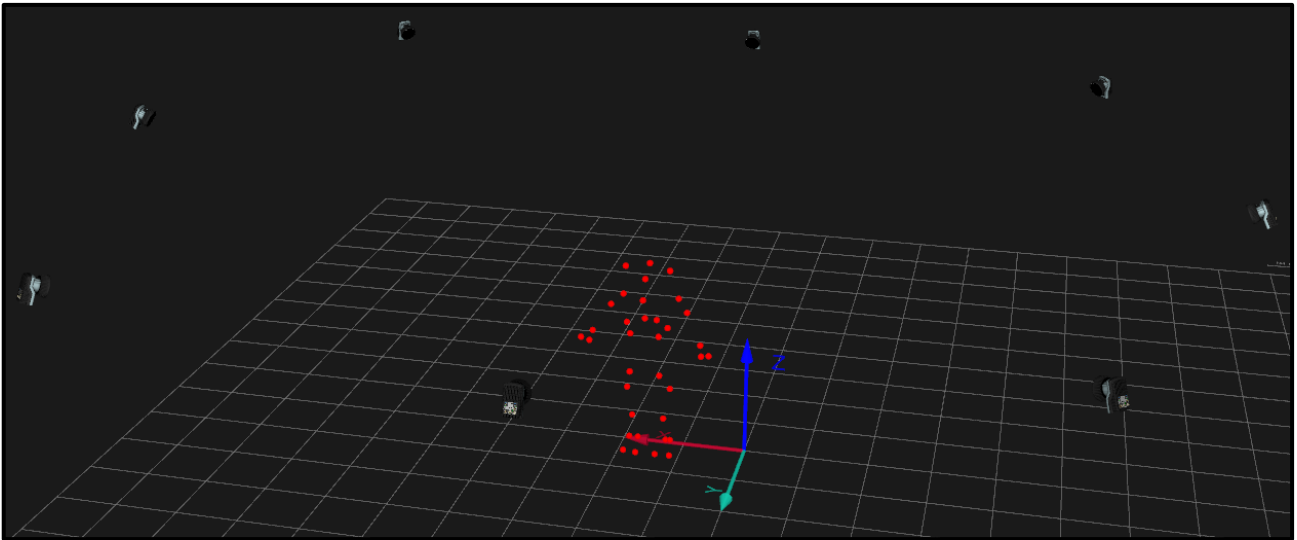
8

Figure 2 - Marker-based motion analysis in Qualisys Track Manager 2.9 (Qualisys, Gothenburg, Sweden), illustrating eight infrared cameras tracking the position of 35 reflective markers placed on the subject and the global reference frame.

Typically, the three translational and rotational DOF can be described as three Cartesian coordinates (X, Y and Z) and three angles of rotation (Euler angles), respectively. Subsequently, the orientation of each segment can be established by embedding a local reference coordinate system, which defines the segments' positions in relation to a global reference frame (e.g., laboratory coordinate system). The angular orientation of the segments can be expressed in two different ways, namely the anatomical joint angles and the segment Euler angles. In the AMS, however, the models are typically formulated using a full Cartesian formulation, where a vector composing the translational and rotational coordinates for each segment is used to define the system coordinates (Damsgaard et al., 2006). This includes the formulation of a rotation matrix based on Euler parameters to describe the segments' rotations. A more detailed description of this method was presented in Andersen et al. (2009).

2.1.2 Kinematic analysis in the AnyBody Modeling System

The kinematic analysis in the AMS is performed using the optimisation method presented in Andersen et al. (2009, 2010), which is summarized in the following. These papers outline a local optimisation-based method for parameter identification of determinate and over-determinate mechanical systems from a given motion input, in this case, input obtained through marker-based motion analysis. This means that the motion input is prescribed by determining the position of a set of markers placed on the skin surface and, subsequently, formulating an optimisation problem to find the best possible fit between measured marker trajectories and the corresponding marker-set defined on the musculoskeletal model. In other words, the goal is to impose the measured motion on the musculoskeletal model, where muscle attachment sites, joint locations etc. has already been defined. When applying this optimisation method, the purpose of the kinematic analysis is threefold: 1) By implementing a scaling law, the musculoskeletal model is morphed to

the same size and shape as the subject the motion data was obtained from, 2) the local coordinates of the markers placed on the model are found, and 3) the joint axes of rotations are altered to fit the subjects as well as possible. It should be noted that the mathematical formulations described here are not meant to be exhaustive and only provides an overview of the main steps in the optimisation approach.

To determine the model kinematics, the segmental positions, velocities and accelerations need to be found, which can be denoted as $q(t)$, $\dot{q}(t)$ and $\ddot{q}(t)$, respectively. For a mechanical system subject to holonomic constraints, such as a musculoskeletal model, position analysis can be formulated as a set of m equations:

$$\Gamma \equiv \Gamma(q, t) = 0 \tag{1}$$

The independent constraint equations consist of the constraints associated with the joints between segments and the constraints that describe the motion, i.e., the kinematic drivers. In the case where there are as many constraint equations, m, as there are system unknowns, n, Eq. (1) can be solved numerically and the velocity and acceleration equations can be derived. For velocity analysis, the equations can be expressed as

$$\Gamma_q \dot{q} + \Gamma_t = 0 \tag{2}$$

where the subscript q and t denotes the partial derivative with respect to q and time, respectively. Differentiation of the velocity equations provides the acceleration equations:

$$\Gamma_q \ddot{q} + (\Gamma_q \dot{q})_q \dot{q} + 2\Gamma_{qt} \dot{q} + \Gamma_{tt} = 0 \tag{3}$$

This formulation is, however, only solvable for kinematically determinate systems ($m = n$). When the system becomes over-determinate ($m > n$), the solution to the problem is obtained by re-formulating the equations into a constrained optimisation problem, presuming that it is possible to split Eq. (1) into two sets:

$$\Gamma(q, t) = \begin{pmatrix} \Psi(q, t) \\ \Phi(q, t) \end{pmatrix} \tag{4}$$

This approach results in a set of equations, $\Psi = \Psi(q, t)$, that only has to be solved as well as possible, while the remaining equations, $\Phi = \Phi(q, t)$, have to be fulfilled completely. Specifically, $\Psi = \Psi(q, t)$ contains the marker constraints, specifying that the marker position in the model must be equal to the measured position, and $\Phi = \Phi(q, t)$ contains the joint constraints. By assuming that the constant model

parameters ($\hat{d}$) are known, the solution to Eq. (4) at *N* discrete time steps can be found by solving the following optimisation problem:

$$q_i^* = \arg\min_{q_i} H(\Psi(q_i, \hat{d}, t_i))$$

$$\text{s.t.} \quad \Phi(q_i, \hat{d}, t_i) = 0$$

(5)

for *i* = 1, 2, …, *N*. While the objective function *H* can have many forms, it is required that the choice of function is twice differentiable to *q*. In this case, a weighted least-square objective function is used, which is expressed as

$$H\left(\Psi(q_i, \hat{d}, t_i)\right) = \frac{1}{2}\Psi(q_i, \hat{d}, t_i)^T W(t_i)\Psi(q_i, \hat{d}, t_i)$$

(6)

The next step is to determine the optimal constant model parameters, d^*. Initially, the optimal constant parameters are assumed known, which enables the determination of the optimal system coordinates at time step i, q_i^*, by solving Eq. (4). Subsequently, an optimization problem can be formulated that produces the same optimal system coordinates for each time step and optimal constant parameters over all time steps:

$$\min_{q(t_1), q(t_2), \dots, q(t_n), d} \sum_{i=1}^{N} H(\Psi(q(t_i), d, (t_i))$$

$$s.t. \quad \Phi(q(t_k), d, (t_k) = 0, \ T(d) = 0$$

(7)

for k = 1, 2, …, *N*. In order to solve the optimisation problem in Eq. (7), one needs to 1) calculate a search direction specifying the next step that is closer to the solution and 2) select a step length in the selected search direction. For further details about the mathematical procedures for determining these variables, please refer to Andersen et al. (2010).

In summary, the overall solution algorithm can be written out as follows. First, the user must specify an initial guess for the system coordinates at the first sample and the constant model parameters. Second, the optimisation problem in Eq. (5) is solved in order to find a new set of initial system coordinates that can be used to solve the optimisation problem in Eq. (7). Third, the optimisation problem in Eq. (7) is solved, which includes calculating the search direction and the step length as described above.

The implementation of this optimisation method to perform kinematic analysis of a musculoskeletal model can be summarized as follows. The equations specifying the difference between measured marker trajectories and the markers positioned on the musculoskeletal model are assigned to $\Psi = \Psi(q,t)$, while the joint constraints and the constraints on the Euler parameters are assigned to $\Phi = \Phi(q,t)$. This means that the difference between marker positions only has to be as small as possible while the model constraints are fulfilled completely, as mentioned previously. In the model, a subset of markers are fixed to bony landmarks on the model bone geometry while the remaining markers are treated as unknowns and optimised. In general, the amount of fixed markers has to be enough to define all model DOF. Additionally, which markers to fix to the bone geometry are chosen by identifying which markers that should define the segment lengths and the joint rotation axes. Based on the position of these markers, the segment lengths are scaled applying a length-mass-scaling law (Rasmussen et al., 2005), which define the new model dimensions and thus the location of joint centres as well as the position of the fixed and optimised markers on the model. As a result, the musculoskeletal model is approximately the same size as the subject it represents and the measured motion has been imposed on the model as well as possible, considering the importance of individual marker positions for defining internal skeletal landmarks.

2.2 Kinetics

Given that the motion of the mechanical system is defined in detail, along with the external forces and boundary conditions, the equations of motion can in principle be solved to provide the internal forces (Rasmussen et al., 2001; Vaughan et al., 1999). However, dynamic equilibrium is not easily obtained when the mechanical system of interest is the musculoskeletal system. In fact, the human body is statically indeterminate, as there are more muscles available than necessary to produce a given motion. This means that there a not enough equilibrium equations to uniquely determine the unknown muscle- and joint forces and, therefore, equilibrium can be obtained by infinitely many solutions. As described by Rasmussen et al. (2001), this statically indeterminacy is normally resolved by the CNS, which chooses a set of muscle actions that produce the desired motion. Because the CNS is able to repeat motions with considerable precision, it has been hypothesized that the recruitment of muscles must be based on a rational criterion. Therefore, the general assumption is that the muscles are recruited based on some kind of optimality condition (Damsgaard et al., 2006), which is specified in the following. The descriptions in section 2.2.1 and 2.2.3 are based on Damsgaard et al. (2006) and Rasmussen et al. (2001), which outline the IDA in the AMS and a more detailed discussion on the choice of muscle recruitment criterion, respectively, as well as the AMS reference manual (AnyBody Technology A/S, Aalborg, Denmark).

2.2.1 Muscle recruitment

The fundamental problem is that there are more muscles available then there are DOF, meaning that there are infinitely many possible muscle recruitment patterns that are acceptable to balance a given load. This indeterminacy can be mathematically interpreted by viewing the total system of equilibrium equations, which can be expressed as

$$Cf = h \tag{8}$$

where C is a matrix of coefficients describing the current position of the body segments, f is a vector comprising all unknown forces and h represents all known forces, i.e., external and inertial forces. Statically indeterminacy means that f contains more elements than there are equations in the formula and the system has infinitely many solutions. However, by assuming that the CNS attempts to minimize the load on the muscles and body, the solution to the unknown muscle and joint forces can be found using an optimization problem. In general, the optimization problem can be expressed as

$$\min \quad G\big(f^{(M)}\big) \tag{9}$$

$$s.t. \quad Cf = h \tag{10}$$

$$0 \leqslant f_i^{(M)} \leqslant S_i, \qquad i \in \big\{1,\dots,n^{(M)}\big\} \tag{11}$$

where G is the assumed criterion of the recruitment strategy and $f^{(M)}$ the unknown muscle forces. The goal is to minimize the objective function G in relation to all unknown forces in the problem, while the dynamic equilibrium equations, Eq. (8), serves as constraints into the optimization. The non-negativity constraints on the muscle forces in Eq. (11) expresses that the muscles can only pull and their capabilities are determined by an upper bound limit, S_i, which, typically, states some measure of muscle strength.

While this optimization problem outlines the general approach for solving the muscle recruitment problem, the objective function G has many forms. In the AMS, there are several options available for the objective function, including *Linear*, *Quadratic*, *Polynomial*, *Min/max or even multiple combinations Muscle Recruitment*. The main things to consider when choosing a criterion are that is has to be physiologically reasonable and fairly efficient computationally. It is not definitively known which criterion that corresponds closest to the actual recruitment strategy of the CNS, but each criterion can be more or less suitable in relation to the specific problem at hand. Linear muscle recruitment is the simplest form of the objective function, which assumes a linear combination of muscle forces, typically, in relation to their maximal strength. This criterion is based on the idea that strong muscles do more work than weak muscles. However, this approach will only recruit the minimum number of muscles to balance the system and the

chosen muscles are typically those that are most suitable for this purpose, considering the combination of their moment arms and strengths. This means that the criterion does not consider muscle synergism, i.e., the load-sharing by simultaneously activated muscles, and is, therefore, not physiologically reasonable. Quadratic muscle recruitment is more likely to distribute the load between several muscles instead of only recruiting the minimum number necessary, and is formulated as

$$G = \sum_i \left(\frac{f_i}{S_i}\right)^2 \tag{12}$$

where S_i is the normalization factor, or upper bound limit, based on some measure of muscle strength. In the present study, the maximal isometric muscle strength was implemented. However, if the loads exceed the defined upper bounds of the muscles' strength capabilities, the criterion in Eq. (12) is not able to provide a solution. Generally, increasing the order of the objective function will lead to higher muscle synergy, i.e., the load is shared by more muscles, a feature that can be exploited to decrease the dependency of the upper bound on the muscle recruitment. Polynomial muscle recruitment comprises the higher orders of Eq. (12), where the third order polynomial criterion is the default setting in the AMS, serving as a reasonable compromise between criterions, and the fifth order is the upper limit. The polynomial criterions can only be considered physiologically reasonable if upper bounds are included, preventing individual muscle forces from exceeding their physiological maximum. These constraints, however, have the unfortunate effect of causing sudden changes in muscle force distribution for increased loads. As mentioned above, the need for these upper limits diminishes as the order of the function increases and the remaining option, the Min/max muscle recruitment criterion, corresponds to increasing the order of the polynomial criterion infinitely. By deploying this criterion, the maximum relative load of any muscle in the system is minimized, corresponding to a minimum fatigue criterion with maximum synergism between muscles. This also means that there is no need for upper bound limits, as no muscle will be overloaded if other muscles can contribute to balance the load instead.

2.2.2 External forces

FPs are the predominant tool for quantifying the external forces acting on the body during locomotion (Nigg, 2006) by exerting an equal and opposite load in response to the load applied by the subject to the ground, i.e., the GRF&Ms (Figure 3) (Manal and Buchanan, 2004). A FP is designed to measure the forces and moments applied to its top surface and are commercially available from several manufactures, such as AMTI (Advanced Mechanical Technology, Inc., Watertown, MA, US), Bertec (Bertec Corp., Columbus, OH, US) and Kistler (Kistler Group, Winterthur, Switzerland). As described by Nigg (2006), FPs use a construction in which a rectangular plate is supported at four points and the force transducers for each axis direction are
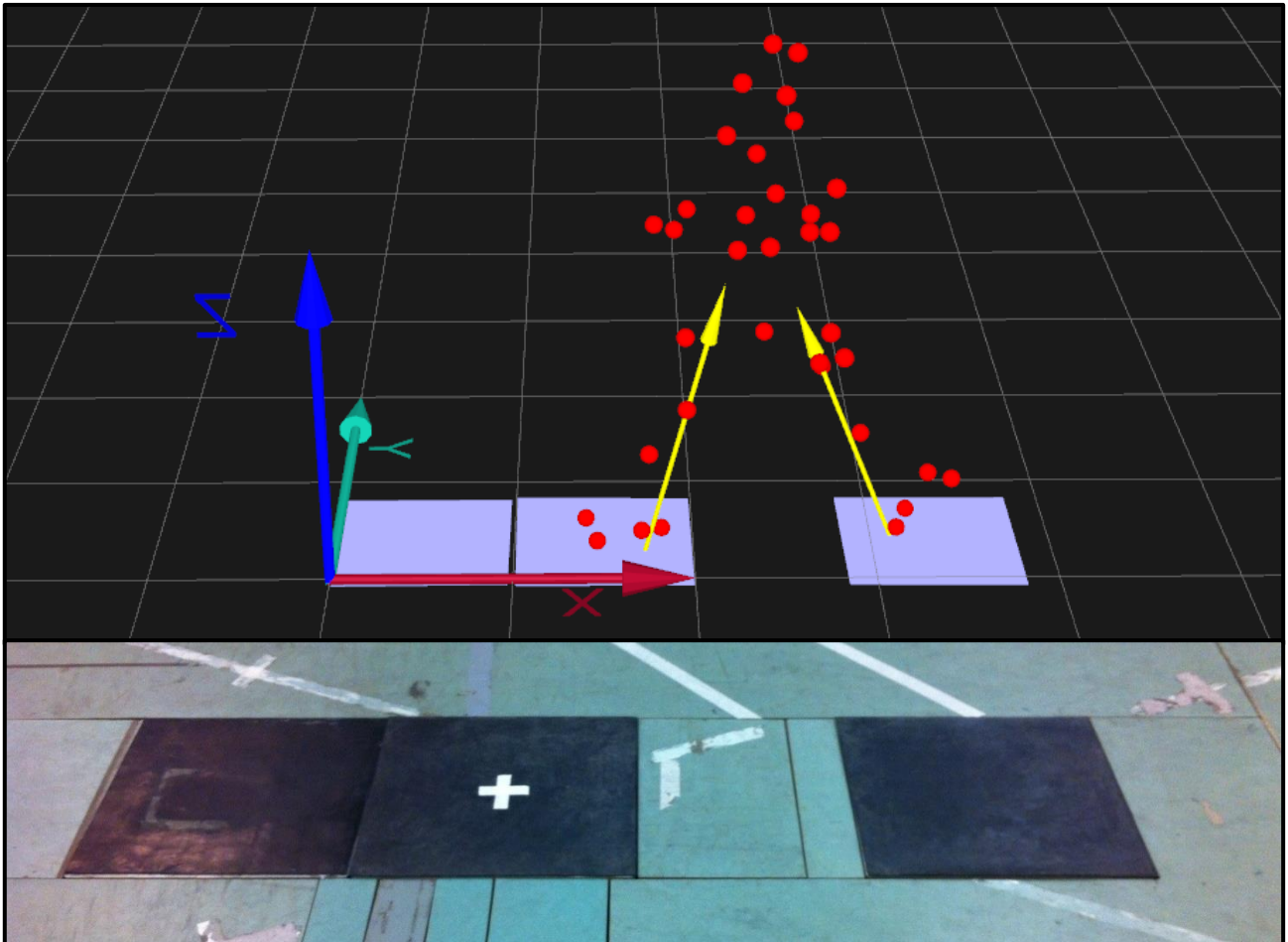
Figure 3 – Three force plates embedded in the laboratory floor (bottom) and a subject impacting the force plates during gait (top), illustrating the ground reaction forces (yellow).

located in each corner. The force transducers typically consist of either piezoelectric or strain gauge transducers, which generates an electrical potential when subjected to mechanical strain. This electrical potential is directly proportional to the magnitude of the applied load (Manal and Buchanan, 2004). In the present study, AMTI FPs are applied to measure the GRF&Ms, incorporating strain gauge force transducers. The most common strain gauge transducers can be classified as either electrical resistance or piezoresistive transducers, which operate similarly with the main difference being the material used (Nigg, 2006). The transducers are mounted on structures that deform if subjected to stress and the geometric change leads to a change in electric conductivity. The resulting change in electric resistance of the structure can be calibrated to provide the corresponding forces. Specifically, the raw analogue data from each FP channel is stored and, subsequently, scaled using analogue scale parameters and a calibration matrix specific to the FP model (Cramp, 2015). This means that the resulting channel outputs can be interpreted directly as three forces (F_x, F_y and F_z) and three moments (M_x, M_y and M_z).

As described by Manal and Buchanan (2004), the GRF&Ms are measured about the X, Y and Z-axis specific to the FP, which, generally, differs from the orientation of the global reference frame of the object-space. Therefore, the GRF&Ms have to be transformed into the appropriate reference system for the subsequent calculation, i.e., to the segment coordinate system where the force is applied. In addition, the FP data must be synchronised with the kinematic observations, specifying the ratio between the sampling frequencies of the FP and the camera-system.

2.2.3 Solving the equations of motion

When the kinematics of the mechanical system has been solved, as described in section 2.1.2, and the external forces obtained, the internal forces and moments are calculated by solving the equations of motion in the form stated in Eq. (8). The position of each segment, or ith body, are described by the coordinates $q_i = \begin{bmatrix} r_i^T & p_i^T \end{bmatrix}$, where r_i is the global position vector of the COM and p_i is a vector comprising the Euler parameters. The segmental velocities can be defined as $v_i = \begin{bmatrix} \dot{r}_i^T & \omega'^T_i \end{bmatrix}$, where ω'_i is the angular velocity in relation to the segment's local reference frame. The kinematic analysis provided a solution to a set of imposed kinematical constraints in the form

$$\Phi(q, t) = 0 \tag{13}$$

where $q = \begin{bmatrix} q_1^T \dots q_n^T \end{bmatrix}$ represents the assembled coordinate vector for all n segments. Subsequently, the linear velocity and acceleration constraints was solved in terms of v and $\dot{v}$:

$$\Phi_{q^*} v = -\Phi_t \quad \text{and} \quad \Phi_{q^*} \dot{v} = \gamma(q, v, t) \tag{14}$$

where q^* contains a virtual set of positions that correspond to v and Φ_{q^*} is a Jacobian constraint with respect to q^*. For each segment, the Newton-Euler equations can be formulated in the form

$$\begin{bmatrix} m_i \mathrm{I} & 0 \\ 0 & \mathrm{J}'_i \end{bmatrix} \dot{v}_i + \begin{bmatrix} 0 \\ \widetilde{\omega}'_i \mathrm{J}'_i \omega'_i \end{bmatrix} = g_i \tag{15}$$

where m_i and J'_i are the segment mass and the matrix of inertia properties in relation to the centroidal segment-frame, respectively. g_i represent the forces, consisting of muscle forces, $g_i^{(M)}$, reaction forces, $g_i^{(R)}$, and known applied forces, $g_i^{(\mathrm{app})}$. $g_i^{(M)}$ and $g_i^{(R)}$ are included in the left-hand side of Eq. (8) while all other variables in Eq. (15) are included in the right hand side, h_i. Therefore, the full right-hand side of Eq. (8) is assembled as $h = \begin{bmatrix} h_1^T \dots h_n^T \end{bmatrix}$, where

$$h_i = g_i^{(\text{app})} - \begin{bmatrix} m_i I & 0 \\ 0 & J'_i \end{bmatrix} \dot{v}_i - \begin{bmatrix} 0 \\ \tilde{\omega}'_i J'_i \omega'_i \end{bmatrix} \tag{16}$$

For the next step, the coefficient matrix, C, is divided according to muscle and reaction forces, $C = [C^{(\text{M})} \quad C^{(\text{R})}]$, which define $g^{(\text{M})} = C^{(\text{M})} f^{(\text{M})}$ and $g^{(\text{R})} = C^{(\text{R})} f^{(\text{R})}$. In order to determine the muscle coefficient matrix, $C^{(\text{M})}$, a model of the muscle geometry must be defined. In this case, the muscles are modelled as elastic strings spanning between two or more points that may wrap over rigid obstacles or other soft tissues. In a simple case without muscle wrapping, the muscle's *origin-insertion length* can be expressed as $l^{(oi)} = \left| r_i^{(\text{p})} \quad r_j^{(\text{p})} \right|$, where $r_i^{(\text{p})}$ and $r_j^{(\text{p})}$ are the positions of the points spanned by the muscle, which depend on q. All modelled muscle paths must provide this length as a function of $l^{(oi)}(q)$ as well as its time-derivative in order to calculate muscle strength, S_i. In accordance with the principle of virtual work, the coefficients in $C^{(\text{M})}$ are the derivatives of $l^{(oi)}$ for the system coordinates in q^*, which are denoted by $l_{i,q^*}^{(oi)}$. Hereby, the virtual work produced by the muscles can be expressed as the sum of muscle forces times their virtual change in length:

$$\delta W = \sum_{i=1}^{n^{(\text{M})}} \delta \, l_{i,q^*}^{(oi)} f_i^{(\text{M})} = \delta q^{*\text{T}} \sum_{i=1}^{n^{(\text{M})}} \delta \, l_{i,q^*}^{(oi)} f_i^{(\text{M})} = \delta q^{*\text{T}} \left[l_{1,q^*}^{(oi)} \, \dots \, l_{n^{(\text{M})},q^*}^{(oi)} \right] \tag{17}$$

Furthermore, the same virtual work can be expressed as the scalar product of the generalized force vector for all muscles, $g^{(\text{M})}$, and the virtual change of the system coordinates, q^*:

$$\delta W = \delta q^{*\text{T}} g^{(\text{M})} = \delta q^{*\text{T}} C^{(\text{M})} f^{(\text{M})} \tag{18}$$

At this point, all inputs to the system equations, i.e., the equations of motion (Eq. (8)) and the muscle recruitment problem (Eq. (9) and (11)), have been established and the equations can be solved to provide the muscle and joint reaction forces as well as the joint moments from a given motion input.

3. Errors associated with experimental input data

The accuracy of the estimates provided by IDA is highly dependent on the quality of the data that is used as input to the equations of motion (Pámies-Vila et al., 2012; Riemer et al., 2008). As described by Kuo (1998), these data are generally not known exactly and their precision often comes with considerable expense. However, inaccuracies to any of these input variables can cause dynamic inconsistency, a condition where residual forces and moments are introduced in the model to achieve dynamic equilibrium.

3.1 Estimating body segment parameters

While it is well-established that the different methods for estimating BSPs yields different results, the influence of varying BSP values in the resulting model kinetics is less clear (Rao et al., 2006; Silva and Ambrósio, 2004; Pearsall and Costigan, 1999). Pearsall and Costigan (1999) compared the BSP estimations of different predictive functions found in the literature, which resulted in up to 40 % variation in mass and MOI values. However, while the different estimation models statistically affected almost half the kinetic measures, the effects were less than 1 % of bodyweight. The authors further stated that although the effects seemed relatively small, the BSP estimations are important, as its influence on kinetic measures is likely to increase during movements that require large limb accelerations, such as running. Similarly, Rao et al. (2006) showed that BSP values substantially differ in relation to the BSP estimation model with variations ranging from 9.73 % up to 60 %. The effect of BSP variation on joint kinetics was indecisive, but given the large variation in BSP estimates the authors emphasized that their influence on IDA results should be carefully considered.

3.2 Marker-based motion analysis: Measurement errors and reliability

Due to the popularity of marker-based motion analysis systems and the importance of accurate kinematic measurement for IDA, it is important to assess the reliability and measurement errors of these systems. Today, it is well known that marker-based motion analysis have several limitations and the origin and magnitude of associated measurement errors have been extensively investigated (McGinley et al., 2009; Benoit et al., 2006; Stagni et al., 2005; Chiari et al., 2005; Della Croce et al., 2005; Leardini et al., 2005; Richards, 1999). Most notable are the measurement error or noise associated with the markers sliding with the skin relative to the bones due to intermediate soft tissues, which is known as soft-tissue artefacts (STA) (Andersen et al., 2009; Benoit et al., 2006; Leardini et al., 2005; Stagni et al., 2005). As described by Leardini et al. (2005), several factors contribute independently to STA, such as inertial effects, skin deformation and sliding, mainly occurring near the joints, and deformation caused by muscle contractions. The magnitude of STA errors have been quantitatively assessed in Benoit et al. (2006) and Stagni et al. (2005). Minimizing the contribution of STA and compensating for the effects are fundamental issues for motion analysis and several methods have been proposed, which were reviewed in Leardini et al. (2005). In addition, the marker-based system itself has instrumental errors, causing inaccuracies in the resulting marker coordinates, which can be classified as either systematic or random errors (Chiari et al., 2005). As described by Chiari et al. (2005), systematic errors are associated with the kinematic model of the measurement system, where errors can stem from calibration inaccuracies and/or the inadequacy of this model to take care of non-linarites in the data caused by image distortion. Random errors are caused by factors such as

electronic noise, marker flickering, marker imaged shape distortion, partially obscured marker images, merging of markers with each other or phantom signals.

3.3 Force plates: Instrumental errors and calibration

While the errors associated with acceleration data are well-understood and reduced using dedicated methods, the errors associated with FP measurements typically receive less attention (Psycharakis and Miller, 2006). As described by Psycharakis and Miller (2006), assuming that FP data are acceptably accurate can potentially be problematic, as error associated with the force measurements will propagate through the subsequent calculations of forces and moments, thus affecting the final results. In order to obtain reliable and accurate force measurements, the FP must have adequate system sensitivity, a low force detection threshold, high linearity, low hysteresis and crosstalk, electrical inductance and temperature and humidity variations (Bartlett, 2007). The magnitude of possible measurement errors were established by Psycharakis and Miller (2006). The study showed that although the FP system investigated had low hysteresis, good linearity, and acceptable crosstalk, the estimated maximum error in the resulting vertical force measurements were 8.17 %. Another issue concerns the FP's determination of point-of-force application, which has been associated with considerable errors (Bobbert and Schamhardt, 1990). Bobbert and Schamhardt (1990) reported point-of-force application errors ranging from - 20 to + 20 mm for a static point loading condition and a dynamic trial where a subject ran across the FP, resulting in an estimated between trial error of up to 40 mm. However, Middleton et al. (1999) found that for a stabilometry task, where a subject was standing with both feet placed symmetrically on the plate, the expected error in determining COP are likely to be less than 2 mm. Common for both studies, however, was the result that the COP determination deteriorated substantially near the edges of the plate.

In order to reduce the errors associated with the FP characteristics described above, Bartlett (2007) presented guideline values for each of the FP system requirements described above. By inspecting and implementing these set values to the FP system, the accumulating error from each of these characteristics may be held to an acceptable magnitude. In addition, initial calibration procedures are necessary to ensure that systematic errors in the system are reduced to a point where they can be considered negligible (Payton and Bartlett, 2008; Bartlett, 2007). Usually, the calibration of the amplifier output as a function of force input is set by the manufacturers but may require periodic checking (Bartlett, 2007). As described by Payton and Bartlett (2008) and Bartlett (2007), the vertical force and point-of-force application can be fairly easily calibrated under static loading conditions by placing known weights on the plate at various positions. However, calibration of the other force variables is more challenging and, generally, not possible when the plate has been inserted into the ground. This issue, furthermore, restricts the determination of crosstalk to

the vertical force component. Finally, another issue related to calibration is that the accuracy of determining the COP and free moment depends on operating conditions (Payton and Bartlett, 2008). While the accuracy of the force components depends only on the performance of the individual load cells, COP is affected by the force level, force direction and force location on the plate's surface, which, furthermore, affects the free moment about the vertical axis. Therefore, a constant level of accuracy cannot be established for these variables.

3.4 Overdeterminacy and dynamic inconsistency

When performing IDA, there are two issues that compromise the dynamic consistency: 1) The overdeterminacy of the system when inputting the GRF&Ms to the equations of motion (Hatze, 2002) and 2) the accumulated measurement inaccuracies in the experimental input data (Pámies-Vila et al., 2012; Riemer et al., 2008). As described by Hatze (2002), the fundamental inconsistency stems from the fact that incompatible model input data are used to obtain the desired outputs. Specifically, there exists a mismatch between the measurements taking from the real biosystem and the mathematical model of this system, which inverse dynamical behaviour differs to some extent. An aspect of this mismatch is the overdeterminacy introduced when inputting the GRF&Ms to the equations of motion (Pámies-Vila et al., 2012; Riemer and Hsiao-Wecksler, 2008; Hatze, 2002). By inputting the GRF&Ms, a boundary condition for the bottom-most segment is formed, which results in redundant information as there are now more equilibrium equations than system unknowns. Typically, the overdeterminacy of the system can be avoided by either discarding acceleration measurements for the top-most segment or by adding residual forces and torques to the top-most segment (Kuo, 1998). Furthermore, the accumulation of measurement errors in the experimental input data contributes to the dynamic inconsistency of the model and thus the magnitude of the residual forces and moments (Pámies-Vila et al., 2012; Riemer et al., 2008).

As described by Riemer and Hsiao-Wecksler (2008), this redundancy of forces and moments has been used to reduce error effects from the input data through optimization methods, aimed towards minimizing these residuals. This means that specific input parameters are adjusted in the top-down calculations until the difference between measured GRF data and the GRF predicted by the top-down approach are minimized. To accomplish this, several optimization methods have been proposed that adjusts BSPs (Vaughan et al., 1982), joint accelerations (Cahouët et al., 2002) and angular position data (Riemer and Hsiao-Wecksler, 2008) or, for example, a least-squared optimization approach that finds the most agreeable joint torques in relation to the available measurement data for each point in time (Kuo, 1998).

However, another solution for solving the overdeterminacy issue and improve the dynamic consistency of the model is to further develop the top-down approach, where GRF&Ms are calculated from

the equations of motion. The fundamental issue that has limited the application of the top-down approach for many purposes is the indeterminacy arising from a so-called double contact phase, where more than one segment is in contact with the environment and the system forms a closed kinetic chain (Fluit et al., 2014). However, in recent years, several studies have presented solutions to this issue, which enables the prediction of GRF&Ms under both feet during tasks involving a double contact phase (Fluit et al., 2014; Choi et al., 2013; Eel Oh et al., 2013; Ren et al., 2008; Audu et al., 2007).

4. Prediction of ground reaction forces

By predicting the GRF&Ms, several limitations associated with the use of measured GRF&Ms from FPs can potentially be overcome. First, the residual forces and moments resulting from the overdeterminacy in the current approach can be reduced, as the GRF&Ms are adjusted according to the other measurement data. Second, when subjects are required to impact FPs during measurements, the analysis of movements that are continuous and occupy a large space is very limited (Choi et al., 2013). Third, it is often necessary to install the FPs in a fixed space in order to obtain reliable measurements, usually within a laboratory, which means that the application of FPs outside controlled environments are currently infeasible (Choi et al., 2013; Eel Oh et al., 2013). Fourth, FP data is associated with errors that can affect the final results of the analysis, as described in section 3.3, which would be advantageous to eliminate. Finally, during gait or running analysis for instance, segment angles and GRF&Ms can be altered if subjects attempt to modify their movement pattern in order to ensure FP contact (Challis, 2001). In the following, the different approaches for predicting the GRF&Ms during double contact phase are summarized.

Audu et al. (2003) used an optimization method to compute GRF&Ms during different static postures in a human bipedal standing model. The optimization method was based on the assumption that during quiet stance, the ground reaction force would be located in a position under the foot, minimizing all the lower extremity joint moments that are required to maintain such a posture. Therefore, the indeterminacy problem was solved by letting one foot be in contact with the ground and estimating the location and magnitude of the ground reaction forces needed at the other foot thus solving the problem as an open-kinetic chain. The method was validated against measured data in Audu et al. (2007) for an array of static standing postures, but it is unknown if the method can be used for dynamic movements. Ren et al. (2008) proposed a *Smooth Transition Assumption* to predict GRF&Ms during double contact based on the use of simple functions that closely followed measured FP data. The analytical functions were determined by trial and error until good matches to experimental data were established. While the approach provided reasonably good estimates of sagittal plane GRF&Ms, it required experimental data to formulate the

analytical functions, which makes it unclear whether this approach is valid for other movements. Eel Oh et al. (2013) and Choi et al. (2013) applied a data learning based artificial neural network model to solve the indeterminacy problem. During gait, correlation coefficients ranging from 0.990-0.965 for the force components and 0.809-0.986 for the moments were established between measured and predicted GRF&Ms. However, the artificial neural network also required large amounts of experimental data, which are not always available, and the predictive ability of this method was highly depended on a suitable selection of input variables.

Most recently, Fluit et al. (2014) demonstrated a universal method for predicting GRF&Ms based on measured kinematic data only, in which the indeterminacy issue was solved without the use of empirical or training data. This was accomplished by introducing five artificial muscle-like actuators at 12 contact points under each foot of a musculoskeletal model and computing the GRF&Ms as part of the muscle recruitment algorithm, as described in section 2.2.1. More specifically, the skeletal muscles and muscle-like actuators were weighted equally in the muscle recruitment algorithm, which minimized the sum of the cubed muscle activations. The method was validated against measured data for an array of activities of daily living, such as gait, deep squatting and stair ascent, and reasonably good results were obtained for all analysed activities. For example, the model showed excellent predictions of vertical ground reaction force for almost all activities with correlation coefficients ranging from 0.621 – 0.980 (median 0.957). However, it has not been investigated whether similar results can be obtained during more dynamic movements, which are particularly relevant for sports science research.

5. References

Andersen, M. S., Damsgaard, M., MacWilliams, B. & Rasmussen, J. 2010, "A computationally efficient optimisation-based method for parameter identification of kinematically determinate and over-determinate biomechanical systems", *Comput. Methods Biomech. Biomed. Engin.,* vol. 13, no. 2, pp. 171–183.

Andersen, M. S., Damsgaard, M. & Rasmussen, J. 2009, "Kinematic analysis of over-determinate biomechanical systems", *Comput. Methods Biomech. Biomed. Engin.*, vol. 12, no. 4, pp. 371–384.

Anderson, F. C. & Pandy, M. G. 2001, "Dynamic optimization of human walking", *J. Biomech. Eng.*, vol. 123, no. 5, pp. 381-190.

The AnyBody Modeling System (Version 6.05) (2015). [Computer software]. Aalborg, Denmark: AnyBody Technology. Available from http://www.anybodytech.com

Arnold, A. S. & Delp, S. L. 2005, "Computer modeling of gait abnormalities in cerebral palsy: application to treatment planning", *Theor. Issues Ergon. Sci.*, vol. 6, no. 3-4, pp. 305–312.

Audu, M. L., Kirsch, R. F. & Triolo, R. J. 2007, "Experimental verification of a computational technique for determining ground reactions in human bipedal stance", *J. Biomech.*, vol. 40, no. 5, pp. 1115–1124.

Audu, M. L., Kirsch, R. F. & Triolo, R. J. 2003, "A computational technique for determining the ground reaction forces in human bipedal stance", *J. Appl. Biomech.*, vol. 19, no. 4, pp. 361–371.

Barret, R. S., Besier, T. F. & Lloyd, D. G. 2007, "Individual muscle contributions to the swing phase of gait: An EMG-based forward dynamics modelling approach", *Simul. Model. Pract. Th.*, vol. 15, no. 9, pp. 1146-1155.

Bartlett, R. M. 2007, *Introduction to sports biomechanics: analysing human movement patterns, second edition*, Abingdon, United Kingdom: Routledge.

Benoit, D. L., Ramsey, D. K., Lamontagne, M., Xu, L., Wretenberg, P. & Renström, P. 2006, "Effect of skin movement artifact on knee kinematics during gait and cutting motions measured in vivo", *Gait Posture*, vol. 24, no. 2, pp. 152–164.

Bobbert, M. F. & Schamhardt, H. C. 1990, "Accuracy of determining the point of force application with piezoelectric force plates", *J. Biomechanics*, vol. 23, no. 7, pp. 705-710.

Boyd, S. & Vandenberghe, L. 2004, *Convex Optimization*, Cambridge, United Kingdom: Cambridge University Press.

Cahouët, V., Luc, M. & David, A. 2002, "Static optimal estimation of joint accelerations for inverse dynamics problem solution", *J. Biomech.*, vol. 35, no. 11, pp. 1507–1513.

Cappozzo, A., Della Croce, U., Leardini, A. & Chiari, L. 2005, "Human movement analysis using stereophotogrammetry. Part 1: theoretical background", *Gait Posture*, vol. 21, no. 2, pp. 186–196.

Carbone, V., Fluit, R., Pellikaan, P., van der Krogt, M. M., Jansen, D., Damsgaard, M., Vigneron, L., Feilkas, T., Koopman, H. F. J. M., Verdonschot, N. 2015, "TLEM 2.0 - A comprehensive musculoskeletal geometry dataset for subject-specific modeling of lower extremity", *J. Biomech.*, vol. 48, no. 5, pp. 734-741.

Challis, J. H. 2001, "The variability in running gait caused by force plate targeting", *J. Appl. Biomech.*, vol. 17, no. 1, pp. 77–83.

Chiari, L., Croce, U. D., Leardini, A. & Cappozzo, A. 2005, "Human movement analysis using stereophotogrammetry. Part 2: Instrumental errors", *Gait Posture*, vol. 21, no. 2, pp. 197–211.

Choi, A., Lee, J.-M. & Mun, J. H. 2013, "Ground reaction forces predicted by using artificial neural network during asymmetric movements", *Int. J. Precis. Eng. Manuf.*, vol. 14, no. 3, pp. 475–483.

Clauser, C. E., McConville, J. T. & Young, J. W. 1969, "Weight, volume, and center of mass of segments of the human body", DTIC Document.

Contini, R., Drillis, R. J., Bluestein, M. 1963, "Determination of body segment parameters", *Hum. Factors J. Hum. Factors Ergon. Soc.*, vol. 5, no. 5, pp. 493–504.

Cramp, E. 2015. *c3d.org*. [ONLINE] Available at http://c3d.org. [Accessed 23 May 15].

Damsgaard, M., Rasmussen, J., Christensen, S. T., Surma, E. & de Zee, M. 2006, "Analysis of musculoskeletal systems in the AnyBody Modeling System", *Simul. Model. Pract. Theory*, vol. 14, no. 8, pp. 1100–1111.

Della Croce, U., Leardini, A., Chiari, L. & Cappozzo, A. 2005, "Human movement analysis using stereophotogrammetry. Part 4: assessment of anatomical landmark misplacement and its effects on joint kinematics", *Gait Posture*, vol. 21, no. 2, pp. 226–237.

Delp, S. L., Anderson, F. C., Arnold, A. S., Loan, P., Habib, A., John, C. T., Guendelman, E. & Thelen, D. G. 2007, "OpenSim: Open-Source Software to Create and Analyze Dynamic Simulations of Movement", *IEEE Trans. Biomed. Eng.*, vol. 54, no. 11, pp. 1940–1950.

Delp, S. L. & Loan, J. P. 1995, "A graphics-based software system to develop and analyze models of musculoskeletal structures", *Comput. Biol. Med.*, vol. 25, no. 1, pp. 21-34.

Eel Oh, S., Choi, A. & Mun, J. H. 2013, "Prediction of ground reaction forces during gait based on kinematics and a neural network model", *J. Biomech.*, vol. 46, no. 14, pp. 2372–2380.

Erdemir, A., McLean, S. & Herzog, W. 2007, "Model-Based Estimation of Muscle Forces Exerted during Movements", *Clin. Biomech.*, vol. 22, no. 2, pp. 131-154.

Ferrari, A., Benedetti, M. G., Pavan, E., Frigo, C., Bettinelli, D., Rabuffetti, M., Crenna, P. & Leardini, A. 2008, "Quantitative comparison of five current protocols in gait analysis", *Gait Posture*, vol. 28, no. 2, pp. 207–216.

Fluit, R., Andersen, M. S., Kolk, S., Verdonschot, N. & Koopman, H. F. J. M. 2014, "Prediction of ground reaction forces and moments during various activities of daily living", *J. Biomech.*, vol. 47, no. 10, pp. 2321–2329.

Fong, D. T.-P. & Chan, Y.-Y. 2010, "The Use of Wearable Inertial Motion Sensors in Human Lower Limb Biomechanics Studies: A Systematic Review", *Sensors*, vol. 10, no. 12, pp. 11556–11565.

Frantz, D. D., Wiles, A. D., Leis, S. E. & Kirsch, S. R. 2003, "Accuracy assessment protocols for electromagnetic tracking systems", *Phys. Med. Biol.*, vol. 48, no. 14, pp. 2241-2251.

Ganley, K. J. & Powers, C. M. 2004, "Determination of lower extremity anthropometric parameters using dual energy X-ray absorptiometry: the influence on net joint moments during gait", *Clin. Biomech.*, vol. 19, no. 1, pp. 50–56.

Hatze, H. 2002, "The fundamental problem of myoskeletal inverse dynamics and its implications", *J. Biomech.*, vol. 35, no. 1, pp. 109–115.

Herzog, W. 2006. Muscle. In: NIGG, B. M. & HERZOG, W. (ed.) *Biomechanics of the Musculo-skeletal System, Third Edition*. Chichester, England: John Wiley & Sons Ltd.

Huston, R. L. 2009, *Principles of Biomechanics*, Boca Raton, Florida, USA: CRC Press.

Horsman, M. D. K., Koopman, H. F. J. M., van der Helm, F. C. T., Prosé, L. P., Veeger, H. E. J. 2007, "Morphological muscle and joint parameters for musculoskeletal modelling of the lower extremity", *Clin. Biomech.*, vol. 22, no. 2, pp. 239–247.

Kuo, A. D. 1998, "A least-squares estimation approach to improving the precision of inverse dynamics computations", *J. Biomech. Eng.*, vol. 120, no. 1, pp. 148-159.

Leardini, A., Chiari, L., Croce, U. D. & Cappozzo, A. 2005, "Human movement analysis using stereophotogrammetry. Part 3. Soft tissue artifact assessment and compensation", *Gait Posture*, vol. 21, no. 2, pp. 212–225.

Luinge, H. J. & Veltink, P. H. 2005, "Measuring orientation of human body segments using miniature gyroscopes and accelerometers", *Med. Biol. Eng. Comput.*, vol. 43, no. 2, pp. 273–282.

Lund, M. E., Andersen, M. S., de Zee, M. & Rasmussen, J. 2015, "Scaling of musculoskeletal models from static and dynamic trials", *Int. Biomech.*, vol. 2, no. 1, pp. 1–11.

Lund, M. E., de Zee, M., Andersen, M. S. & Rasmussen, J. 2012, "On validation of multibody musculoskeletal models", *Proc. Inst. Mech. Eng. [H]*, vol. 226, no. 2, pp. 82–94.

Manal, K.T. & Buchanan, T. S. 2004. Biomechanics of Human Movement. In: KUTZ, M. (ed.) *Standard Handbook of Biomedical Engineering and Design*, New York, USA: McGraw-Hill.

Marra, M. A., Vanheule, V., Fluit, R., Koopman, B. H. F. J. M., Rasmussen, J., Verdonschot, N. & Andersen, M. S. 2015, "A subject-specific musculoskeletal modeling framework to predict in vivo mechanics of total knee arthroplasty", *J. Biomech. Eng.*, vol. 137, no. 2, 020409.

McGinley, J. L., Baker, R., Wolfe, R. & Morris, M. E. 2009, "The reliability of three-dimensional kinematic gait measurements: A systematic review", *Gait Posture*, vol. 29, no. 3, pp. 360–369.

Mellon, S. J., Grammatopoulos, G., Andersen, M. S., Pegg, E. C., Pandit, H. G., Murray, D. W. & Gill, H. S. 2013, "Individual motion patterns during gait and sit-to-stand contribute to edge-loading risk in metal-on-metal hip resurfacing", *Proc. Inst. Mech. Eng. H J. Eng. Med.*, vol. 227, no. 7, pp. 799-810.

Mellon, S. J., Grammatopoulos, G., Andersen, M. S., Pandit, H. G., Gill, H. S. & Murray, D. W. 2015, "Optimal acetabular component orientation estimated using edge-loading and impingement risk in patients with metal-on-metal hip resurfacing arthroplasty", *J. Biomech*, vol. 48, no. 2, pp. 318-323.

Middleton, J., Sinclair, P. & Patton, R. 1999, "Accuracy of centre of pressure measurement using a piezoelectric force platform", *Clin. Biomech.*, vol. 14, no. 14, pp. 357–360.

Nigg, B. M, Herzog, W. & van den Bogert, A. J. 2006. Modelling. In: NIGG, B. M. & HERZOG, W. (ed.) *Biomechanics of the Musculo-skeletal System, Third Edition*. Chichester, England: John Wiley & Sons Ltd.

Nigg, B. M. 2006. Force. In: NIGG, B. M. & HERZOG, W. (ed.) *Biomechanics of the Musculo-skeletal System, Third Edition*. Chichester, England: John Wiley & Sons Ltd.

Otten, E. 2003, "Inverse and forward dynamics: models of multi-body systems", *Philos. Trans. R. Soc. B Biol. Sci.*, vol. 358, no. 1437, pp. 1493–1500.

Pàmies-Vilà, R., Font-Llagunes, J. M., Cuadrado, J. & Alonso, F. J. 2012, "Analysis of different uncertainties in the inverse dynamic analysis of human gait", *Mech. Mach. Theory*, vol. 58, pp. 153–164.

Pandy, M. G. 2001, "Computer modeling and simulation of human movement", *Annu. Rev. Biomed. Eng.*, vol. 3, no. 1, pp. 245–273.

Payton, C. J. & Bartlett, R. M. 2008, *Biomechanical evaluation of movement in sport and exercise*, Abingdon, United Kingdom: Routledge.

Pearsall, D. J. & Costigan, P. A. 1999, "The effect of segment parameter error on gait analysis results", *Gait Posture*, vol. 9, no. 3, pp. 173–183.

Peebles, L. & Norris, B. 1998, *Adultdata: the handbook of adult anthropometric and strength measurements: data for design safety*, London, England: Department of Trade and Industry.

Psycharakis, S. G. & Miller, S. 2006, "Estimation of Errors in Force Platform Data", *Res. Q. Exerc. Sport*, vol. 77, no. 4, pp. 514–518.

Rao, G., Amarantini, D., Berton, E. & Favier, D. 2006, "Influence of body segments' parameters estimation models on inverse dynamics solutions during gait", *J. Biomech.*, vol. 39, no. 8, pp. 1531–1536.

Rasmussen, J., Zee, M. D., Damsgaard, M., Christensen, S. T., Marek, C. & Siebertz, K. (2005), "A general method for scaling musculo-skeletal models", in: *Proceedings of the International Symposium on Computer Simulation in Biomechanics*, Cleveland, OH, US.

Rasmussen, J., Dahlquist, J., Damsgaard, M., de Zee, M. & Christensen, S. T. 2003a, "Musculoskeletal modeling as an ergonomic design method", in: *Proceedings of the XVth Triennial Congress of the International Ergonomics Association and 7th Joint Conference of the Ergonomics Society of Korea/Japan Ergonomics Society*, Seoul, Korea.

Rasmussen, J., Damsgaard, M., Surma, E., Christensen, S. T., de Zee, M. & Vondrak, V. 2003b, "Anybody - a software system for ergonomic optimization", in: *Fifth World Congress on Structural and Multidisciplinary Optimization*, Venice, Italy.

Rasmussen, J., Damsgaard, M. & Voigt, M. 2001, "Muscle recruitment by the min/max criterion—a comparative numerical study", *J. Biomech.*, vol. 34, no. 3, pp. 409–415.

Ren, L., Jones, R. K. & Howard, D. 2008, "Whole body inverse dynamics over a complete gait cycle based only on measured kinematics", *J. Biomech.*, vol. 41, no. 12, pp. 2750–2759.

Richards, J. G. 1999, "The measurement of human motion: A comparison of commercially available systems", *Human Movement Science*, vol. 18, pp. 589-602.

Riemer, R. & Hsiao-Wecksler, E.T. 2008, "Improving joint torque calculations: Optimization-based inverse dynamics to reduce the effect of motion errors", *J. Biomech.*, vol. 41, no. 7, pp. 1503–1509.

Riemer, R., Hsiao-Wecksler, E. T. & Zhang, X. 2008, "Uncertainties in inverse dynamics solutions: A comprehensive analysis and an application to gait", *Gait Posture*, vol. 27, no. 4, pp. 578–588.

Silva, M. P. T. & Ambrósio, J. A. C. 2004, "Sensitivity of the results produced by the inverse dynamic analysis of a human stride to perturbed input data", *Gait Posture*, vol. 19, no. 1, pp. 35–49.

Stagni, R., Fantozzi, S., Cappello, A. & Leardini, A. 2005, "Quantification of soft tissue artefact in motion analysis by combining 3D fluoroscopy and stereophotogrammetry: a study on two subjects", *Clin. Biomech.*, vol. 20, no. 3, pp. 320–329.

Thelen, D. G. & Anderson, F. C. 2006, "Using computed muscle control to generate forward dynamic simulations of human walking from experimental data", *J. Biomech.*, vol. 39, no. 6, pp. 1107-1115.

Vaughan, C. L., Davis, B. L. & O'Connor, J. C. 1999, *Dynamics of Human Gait, Second Edition*, Western Cape, South Africa: Kiboho Publishers.

Vaughan, C. L., Andrews, J. G. & Hay, J. G. 1982, "Selection of body segment parameters by optimization methods", *J. Biomech. Eng.*, vol. 104, no. 1, pp. 38-44.

Weber, T., Al-Munajjed, A. A., Verkerke, G. J., Dendorfer, S. & Renkawitz, T. 2014, "Influence of minimally invasive total hip replacement on hip reaction forces and their orientations", *J. Orthop. Res.*, vol. 32, no. 12, pp. 1680-1687.

Zajac, F. E., Neptune, R. R. & Kautz, S. A. 2003, "Biomechanics and muscle coordination of human walking: part II: lessons from dynamical simulations and clinical implications", *Gait Posture*, vol. 17, no. 1, pp. 1–17.

Zajac, F. E. & Winters, J. M. 1990. Modeling musculoskeletal movement systems: joint and body segmental dynamics, musculoskeletal actuation, and neuromuscular control. In: WINTHERS, J. M. & SAVIO, L.-Y. W. (ed.) *Multiple Muscle Systems: Biomechanics and Movement Organization*. New York, USA: Springer New York.

Zajac, F. E. 1993, "Muscle coordination of movements: a perspective", *J. Biomechanics*, vol. 26, pp. 109-124.

Information for participants

The following information is provided, as you have volunteered to participate in a study aimed towards evaluating the accuracy of predicted ground reaction forces during highly dynamic movements. The experiment is conducted as part of a Master's thesis in Sports Technology at the Department of Health Science and Technology, Aalborg University. The descriptions below contain all the information about the experiment that is relevant for you, which includes a short introduction to the area of research, the experimental procedures, the risks associated with your participation as well as your rights as a participant. It is important that you read and understand the information provided, as you will be required to provide consent, hereby, acknowledging the demands and circumstances associated with your participation. You are most welcome to direct any questions you might have regarding the information in this document to the responsible investigator (contact details below).

Project title

Prediction of ground reaction forces during highly dynamic movements

Investigator

Sebastian Laigaard Skals (stud.cand.scient in Sports Technology, Department of Health Science and Technology, Aalborg University, sskals10@student.aau.dk, + 45 40 63 77 97)

Supervisors

Dr. Michael Skipper Andersen (Associate Professor, Department of Mechanical and Manufacturing Engineering, msa@m-tech.aau.dk)

Miguel Nobre Castro (Ph.D.-student, Department of Mechanical and Manufacturing Engineering, mnc@m-tech.aau.dk)

Time and location

The experiment takes place in the Human Performance Laboratory, Frederik Bajers Vej 7 A2-105, 9220 Aalborg East, at the following times and dates:

Wednesday	April 8th 2015	12.00 am – 22.00 pm
Thursday	April 9th 2015	08.00 am – 22.00 pm
Friday	April 10th 2015	08.00 am – 22.00 pm

Introduction

Marker-based motion analysis and force plate measurements of ground reaction forces (GRF) are commonly used as input for musculoskeletal models in order to estimate muscle-, joint- and ligament forces. However, the dependency on force plate measurements imposes practical limitations during motion analysis studies. The application of force plates substantially restricts movement; as it can be difficult to ensure force plate impact during measurements, especially during highly dynamic movements. Additionally, it is mostly very impractical to apply force plates outside laboratory environments, in which further restrictions are present due to the spatial constraints of the laboratory. For ambulatory measurements or motion capture during treadmill walking, measurements of GRFs require instrumented shoes that are typically bulky or instrumented treadmills that are expensive and technically difficult to develop, respectively. Being able to obtain accurate GRFs without using force plates would provide researchers with many new opportunities for performing motion analysis studies in e.g. workplaces, sports facilities and outdoor environments.

Recently, a study presented a method that enabled musculoskeletal models to predict GRFs using motion analysis data only, which showed comparable results to force plate measurements during various activities of daily living, such as gait and sit-to-stand. This study showed that it is possible to compute accurate GRFs from musculoskeletal models without any input from force plates, hereby, addressing the limitations stated above. However, it is not clear whether this method can provide similar accuracy for highly dynamic movements, such as sprint, side-cut manoeuvres and jumps, particularly relevant for sports science research. Therefore, the purpose of this study is to evaluate the accuracy of this proposed method to predict GRFs during highly dynamic movements by comparing the results to simultaneously obtained force plate measurements.

Experimental procedures

A marker-based motion analysis study is conducted on a variety of highly dynamic movements, which are specified in the following. During measurements, you will exclusively wear tight fitting underwear or running tights, as 29 reflective markers will be placed on your skin, covering all body segments with the exception of the head. Additionally, you will wear a pair of running shoes with three markers placed on each shoe in order to minimize any potential discomfort due to e.g. forceful ground impacts, thus enabling you to execute the movements more naturally. The marker protocol is illustrated in Figure 1. Marker trajectories are recorded using eight infrared high-speed cameras combined with the accompanying software, Qualisys Track Manager 2.10. Ground reaction forces are obtained using three piezoelectric force plates, which are integrated in the laboratory floor.
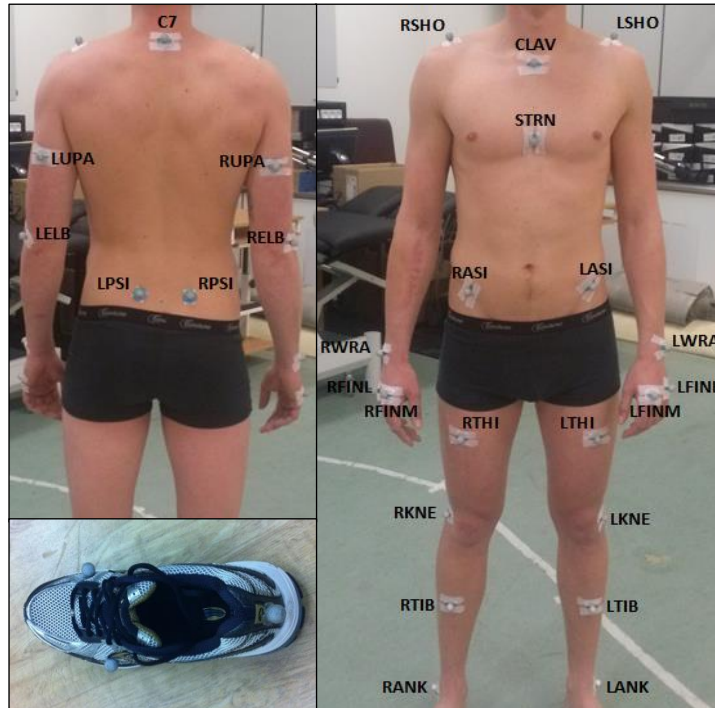
Figure 1 – Marker protocol, illustrating 27 reflective markers placed on the skin and the three markers placed on each running shoe. Two additional markers will be placed on the pelvis, namely the right- and left iliac crest, totalling 35 markers.

Prior to attaching markers, you will be introduced to the experimental procedures and measurements of height and bodyweight will be obtained using measuring tape and a force plate, respectively. Hereafter, you will be asked to complete a warm-up protocol, which involves bicycling at a moderate intensity and practice trials for all the included movements. Initially, you will complete a 5-minute warm-up on a cycle ergometer at an intensity of 160 W. Practice trials are then performed for each movement until you are able to perform the movement satisfactorily while consistently impacting the force plates. After completion of the practice trials, the 29 markers will be taped to your skin.

The following movements are included in the experiment: 1) Gait, 2) running, 3) vertical jump, 4) side-cut, 5) backwards running, 6) jumping from elevated plateau and landing on the dominant leg and 7) accelerate from standing position. Five successful trials will be obtained for each movement, which means that additional repetitions may have to be performed if measurements are incomplete or the movement is performed unsatisfactorily.

Participant inclusion and exclusion criteria

In order to be included in the experiment, participants have to meet the following requirements:

- No abnormalities in bone structure or missing limbs
- No injuries to the lower extremities at the time of data collection

Risks or disadvantages

The majority of the movements included in the study are considered highly dynamic, which means that they are executed at a high velocity and involves forceful ground impacts and sudden changes in direction. However, each trial has a very short duration and will be performed under controlled circumstances and constant supervision. It is assessed that there are no considerable risks or disadvantages associated with your participation. Your comfort and wellbeing will at all times take precedence over the research.

Anonymity

The personal information collected from you, which includes gender, age, height and weight, will not be shared in any way. Your information will be de-identified with a code number, which will be used for any publication purposes. The information that is obtained in connection with this study and can be identified with you will remain strictly confidential and will be disclosed only with your permission.

Accessibility and publication

The data collected will be included in a Master's thesis, which will be made accessible to the public through Aalborg University. Additionally, the results of the study can potentially be published as an article in a scientific journal and/or conference.

Benefits associated with participation

You will not receive any compensation for your participation. While the results of this research may benefit the scientific community, we cannot guarantee that you will receive any personal direct benefits.

Participant rights

Your participation is wholly voluntary and you are free to withdraw your consent and to discontinue participation at any time without prejudice. We will not take responsibility for any accidental injury or discomfort you may experience during the experiment.

Practical information

We kindly ask that you bring a pair of running tights, if accessible, a t-shirt and towel. Female participants will need to bring a sports brassiere. In case you are not able to bring your own, two pairs of tights will be made available for you, however, these may not be of an appropriate size. In addition, we recommend that you bring a water bottle for your own comfort, as the experiment may take up to two hours.

Consent form

Participant name:

_____

I acknowledge that

1) I have read and understood the information provided to me in this document and agree to the general purpose, methods and demands of the study.

2) The project is for the purpose of research and may not be of direct benefit to me.

3) I have been informed that I am free to withdraw from the study at any time without prejudice.

4) My personal information will be treated anonymously and will be disclosed only with my permission.

5) The results of the study will be published by Aalborg University and may, additionally, be published in a scientific journal and/or conference.

6) Participation is wholly voluntary and I will not receive any compensation.

7) I hereby give consent to participate in the study and I am aware that participation is at my own risk.

Participant: **Date:**

_____   _____
(Signature)

Investigator: **Date:**

_____   _____
(Signature)